
COMPARISON OF BAYESIAN METHODS FOR EXTRAPOLATION OF TREATMENT EFFECTS: A LARGE SCALE SIMULATION STUDY

Tristan Fauvel*

Julien Tanniou*

Pascal Godbillot*

Billy Amzal*[†]

ABSTRACT

Extrapolating treatment effects from related studies is a promising strategy for designing and analyzing clinical trials in situations where achieving an adequate sample size is challenging. Bayesian methods are well-suited for this purpose, as they enable the synthesis of prior information through the use of prior distributions. While the operating characteristics of Bayesian approaches for borrowing data from control arms have been extensively studied [1], methods that borrow treatment effects—quantities derived from the comparison between two arms—remain less well understood.

In this paper, we present the findings of an extensive simulation study designed to address this gap. We evaluate the frequentist operating characteristics of these methods, including the probability of success, mean squared error, bias, precision, and credible interval coverage. Our results provide insights into the strengths and limitations of existing methods in the context of confirmatory trials. In particular, we show that the Conditional Power Prior and the Robust Mixture Prior perform better overall, while the test-then-pool variants and the p-value-based power prior display suboptimal performance.

Disclaimer: This document expresses the opinion of the authors of the paper, and may not be understood or quoted as being made on behalf of or reflecting the position of Quinten Health or the European Medicines Agency or one of its committees or working parties.

1 Introduction

Information borrowing from historical or concurrent studies is a promising approach to evaluate medicines for patient populations, such as children or rare diseases patients, in which performing standard randomized controlled trials is difficult. Regulatory agencies are increasingly open to considering methodologies that borrow external information from one or more source populations for the design and analysis of clinical trials through approaches such as Bayesian methods, provided their use is justified. For example, ICH E11 (R1) underscores the ethical imperative to avoid unnecessary pediatric enrollment and suggests leveraging external information in the design and analysis of clinical trials in pediatrics. ICH E11 (R1) was followed by a guideline on pediatric extrapolation (EMA/CHMP/ICH/205218/2022) which provides recommendations, in particular, for using Bayesian statistics in trial design and analysis in the pediatric context. Overall, these guidelines emphasize the need to harmonize methodologies for extrapolation in drug development.

Despite these regulatory advancements, significant gaps remain in understanding the operating characteristics of statistical methods that borrow treatment effects for the design and analysis of clinical trials. The operating characteristics of different Bayesian methods, including the frequentist type 1 error, have been well characterized for borrowing control arm data only [1]. However, when borrowing treatment effects, there is limited understanding of how these characteristics are influenced by key factors such as the drift between source and target treatment effects. This drift is defined as the difference between the expected value of the treatment effect in the target study and the estimate of the treatment effect observed in the source study [2, 3, 4]. Moreover, the comparative performance of different approaches has not been systematically evaluated.

*Quinten Health, 8 rue Vernier, Paris, France

[†]Corresponding author, b.amzal@quinten-health.com

In this work, we perform a large-scale simulation study aimed at evaluating and comparing Bayesian and frequentist methods for borrowing treatment effects in clinical trials under several scenarios. We varied, in particular, the sample size of the clinical trial in the target population, the magnitude of the treatment effect, as well as the parameters needed to specify the models. We then considered the impact of borrowing on the probability of success and other key operating characteristics. By systematically examining the underlying operating characteristics, this study seeks to provide a clearer understanding of how these methods perform across varying settings and parameter choices.

2 Methods

2.1 Scenarios considered

To mimic the situation of pediatric extrapolation, where information on the treatment effect in adults may be used to inform trials in pediatrics, we focus on scenarios where non-concurrent data sources could be used to inform the design and analysis of a target clinical trial. Importantly, no covariates were included.

2.1.1 Selected case studies

To ensure the scenarios considered in the simulation study are realistic, we took inspiration from existing studies in adults and pediatrics. We searched for studies where the efficacy of treatment was assessed in similar settings in adults and in pediatrics, and that cover a variety of endpoints, summary measures, disease areas, and sample sizes. This selection is summarized in Supplementary Table S8.

Botox for the treatment of lower limb spasticity (continuous endpoint) We considered a case study on Botox introduced in Wang, Travis, and Gajewski [5], based on a published phase 3 RCT in 412 pediatric patients to evaluate Botox with standardized physical therapy to treat lower limb spasticity. The primary endpoint was the change in a relevant clinical score. There was not enough evidence to declare the treatment superior to the control, yet Botox was previously approved in adults with a similar indication.

Dapagliflozin for the management of type II diabetes (continuous endpoint) As another case study with a continuous endpoint, we considered the RCT reported in Shehadeh et al. [6], investigating the efficiency of Dapagliflozin for the management of uncontrolled type 2 diabetes in pediatric patients ($N = 81$ in the Dapagliflozin group, $N = 76$ in the placebo group). The primary endpoint was change in HbA(1c) at week 26. Analysis of the data demonstrated the effectiveness of Dapagliflozin. As a source study, we considered a phase 3 trial including adults with type 2 diabetes receiving daily metformin and had inadequate glycemic control [7]. For correspondence between the study in adults and pediatrics, we focused on the arm receiving 5 mg daily Dapagliflozin ($N = 133$) and the placebo arm ($N = 134$). The treatment effect, measured as the difference in mean decrease in HbAc between the two arms, from baseline to week 24 (assumed normally distributed) is 0.36 (95% CI 0.16 to 0.56) [8].

Belimumab for the treatment of seropositive systemic lupus erythematosus (binary endpoint) As a case of binary endpoint, we considered the study of intravenous Belimumab for use in pediatrics aged 5-17 years with active, seropositive systemic lupus erythematosus (SLE) [9, 4]. A pediatric post-marketing RCT in pediatrics was conducted with a total of 92 subjects [10], and a post-hoc Bayesian analysis which borrowed information from the treatment effect in a phase 3 adult study was performed [11]. The data from the two trials in adults are pooled and considered to be one single source of historical data. The pooled odds ratio based on a total of $N_S = 1125$ subjects from these studies was 1.62 (95% CI, 1.27 - 2.05).

Aprepitant for the prevention of postoperative nausea and vomiting (binary endpoint) As another case study with a binary endpoint, we considered the use of Aprepitant for the prevention of postoperative nausea and vomiting in pediatric subjects [12]. An adult trial with sample sizes 293 and 280 in the treatment and control groups showed a response of 63.0% in the treatment group, and 55.0% in the control group. [13]. A similar randomized phase 2b study was completed in pediatrics [14]. The endpoint was the absence of vomiting and the non-use of rescue therapy within 0-24 hours post-surgery. The difference in response rates in the treatment group and control group was 3.4%.

In this case study (in which the treatment effect is a difference in proportions), we followed an approach initially described in Jin and Yin [15], in which a prior is put on the target study control rate (such as a beta prior or a uniform prior in the $[0,1]$ range), and a prior is put on the target study treatment effect (such as a truncated normal).

Teriflunomide for the treatment of Multiple Sclerosis (time-to-event endpoint) As a case study with a time-to-event endpoint, we considered the study on Safety and Efficacy of Teriflunomide vs Placebo in pediatric Multiple Sclerosis (TERIKIDS) [16], which assessed Teriflunomide in pediatrics (57 placebo vs 109 Teriflunomide). Bovis, Ponzano, Signori, Schiavetti, Bruzzi, and Sormani [17] applied a Bayesian approach for estimating the effect of Teriflunomide in pediatrics in the TERIKIDS study, by integrating the available knowledge on Teriflunomide in adults. As source studies, they used published data from 2 randomized clinical trials testing Teriflunomide in adult patients with MS (TEMISO3: 363 placebo vs 359 Teriflunomide O'Connor et al. [18], and TOWER4: 389 placebo vs 372 Teriflunomide Confavreux et al. [19]). The primary endpoint was the time to first relapse, and the treatment effect summary measure was the log hazard ratio for active treatment compared to placebo (assumed to be normally distributed). Bovis, Ponzano, Signori, Schiavetti, Bruzzi, and Sormani [17] pooled hazard ratios (HRs) and 95% CIs on time-to-first relapse (log scale) by inverse of variance weighting. The observed HRs of Teriflunomide on time-to-first relapse in TEMISO, TOWER, and in TERIKIDS were 0.72 (95% CI, 0.58-0.90), 0.63 (95% CI, 0.50-0.79), and 0.66 (95% CI, 0.39-1.11), respectively.

Mepolizumab for the management of severe asthma (recurrent event endpoint) As a case of recurrent event endpoint, we considered a case study described in detail in Best, Price, Pouliquen, and Keene [20], based on a post hoc analysis of the MENSA trial of Mepolizumab in severe asthma [21] by Keene, Best, Price, and Pouliquen [22]. In the MENSA trial, the primary endpoint was the rate of clinically significant exacerbations per year. The summary measure of the treatment effect was the log event rate ratio obtained from negative binomial regression of the observed exacerbation counts (normal approximation) for active treatment compared to placebo. The trial included 25 adolescents (9 control patients) and 551 adult subjects (182 in the control group). The log(RR) in adolescents is -0.40 with standard error 0.703, whereas the log(RR) in adults is -0.69, with a standard error of 0.13 [20]. To determine the rate in the adult control group, we used the data from Ortega et al. [21]. We assumed that the effect of the pediatric subgroup in the overall rate computation is negligible, and therefore set the adult control rate equal to the overall control rate, 1.74. We then computed the rate in the treatment group so as to be consistent with the control rate and the log(RR), that is 0.87.

2.1.2 Sample sizes

For a given case study, the source data sample size N_S was fixed across scenarios, but we varied the target data sample size N_T in a range of values where the maximum is the same as N_S , and the minimum is a much lower value, but still realistic for a trial in pediatrics. We therefore included cases where $N_T = N_S$, $N_T = N_S/2$, $N_T = N_S/4$ and $N_T = N_S/6$. The corresponding sample sizes for each case study are given in Supplementary Table S1. The sample sizes in each arm of the target study were equal.

2.1.3 Drift in treatment effect

The drift in treatment effect is defined as the difference between the expected value of the treatment effect in the new study and the estimate of the source treatment effect, $\delta = \theta_T - \hat{\theta}_S$ [1, 3, 4]. It is the key driver of bias when using extrapolation. We are particularly interested in drift values corresponding to a target treatment effect $\theta_T \in [\theta_0, \hat{\theta}_S]$, where θ_0 is the boundary of the null hypothesis space Θ_0 (drift in $[\theta_0 - \hat{\theta}_S, 0]$). We focused in particular on three scenario categories :

1. the expected value of the effect in the target population is the same as the observed treatment effect in the source population ("consistent treatment effect"),
2. the expected value of the effect in the target population is half that observed in the source population ("partially consistent treatment effect"),
3. there is no treatment effect in the target population.

Where needed, the interval $\theta_T \in [\theta_0, \hat{\theta}_S]$ was extended to properly characterize the OCs of interest. Details on the approach used to calculate extended limits and the specific ranges considered for each use case are provided in the supplementary section A.1 of the supplemental material.

2.1.4 Changes in the denominator of source ratio summary measures

We intended to determine if changes in the denominator value of a ratio-like summary measure (i.e. RR, OR, HR) have an impact on the operating characteristics. To do so, two additional values are considered for the

denominator of the source study summary measures: $1/2$ and $3/2$ of the original study value, while keeping the value of the treatment effect in the source study constant. Such change implies a change in the standard error on the treatment effect in the source study.

2.2 Data generation and sampling approximations

When generating aggregate data for simulated trials, two alternatives can be considered: The first approach is to generate aggregate data following the true data-generating mechanism. Another approach, computationally more efficient in some cases, is to generate the summary aggregate data by assuming a sampling mechanism that matches the likelihood used at the analysis stage (later referred to as "approximate sampling"). The Teriflunomide case study (time-to-event endpoints) is the only case study for which we used approximate sampling in order to gain computational speed. Below, we detail the approaches used for sampling aggregate data for each case study.

2.2.1 Data generation for continuous endpoints

For continuous endpoints, we simply sampled patient-level data from $\mathcal{N}(\hat{\theta}_S + \delta, \sigma_T^2)$. The corresponding summary measures (estimate of the mean and standard error on the mean) were then computed. The target data sampling variance σ_T^2 was set as a scenario parameter. Note that this is not the variance used at the analysis stage. At the analysis stage, we assumed that the target data variance is known, and equal to the empirical variance in the target data sample, $\hat{\sigma}_T^2$.

2.2.2 Data generation for binary endpoints

To generate summary measures that are log odds ratio, we sampled data according to the true data-generating process, that is: $n_T^{(c)} \sim \mathcal{B}(n_T^{(c)} | N_T^{(c)}, p_T^{(c)})$ and $n_T^{(t)} \sim \mathcal{B}(n_T^{(t)} | N_T^{(t)}, p_T^{(t)})$, where :

- n_T^a : number of responders in arm a (c : control, t : target) of the target trial.
- N_T^a : number of subjects in arm a of the target trial.
- $p_T^{(c)}$: response rate in arm a of the target trial.

Then, we computed the corresponding estimated rates : $\hat{p}_T^a = \frac{n_T^a}{N_T^a}$, and finally, the summary measure of the treatment effect: $\hat{\theta}_T = \log \left(\frac{\hat{p}_T^{(t)} / (1 - \hat{p}_T^{(t)})}{\hat{p}_T^{(c)} / (1 - \hat{p}_T^{(c)})} \right)$. Additionally, we estimated the standard error on the treatment effect as: $\hat{\sigma}_{\theta_T} = \sqrt{\frac{1}{n_T^{(c)}} + \frac{1}{N_T^{(c)} - n_T^{(c)}} + \frac{1}{n_T^{(t)}} + \frac{1}{N_T^{(t)} - n_T^{(t)}}}$. We assumed that the response rates are the same in the source and target studies control arms. So, for drift δ , the response rate in the target study treatment arm is: $p_T^{(t)} = \frac{e^\delta}{e^\delta + 1 / \text{odds}_S}$, where odds_S is the observed odds in the source study.

2.2.3 Data generation for time-to-event endpoints

To limit computational time, we used approximate sampling in this case. To do so, we first sample a number of events in each arm a , $n_T^{(a)}$, from $\mathcal{P}(\lambda_T^{(a)} \Delta t N_T^{(a)})$, where Δt is the maximum follow-up time. $\lambda_T^{(c)}$ and $\lambda_T^{(t)}$ are the rates in the control arm and treatment arm of the target study, respectively. We then sampled summary measures of the treatment effect from $\mathcal{N} \left(\log(\lambda_T^{(t)} / \lambda_T^{(c)}), \sqrt{\frac{1}{n_T^{(t)}} + \frac{1}{n_T^{(c)}}} \right)$. Note that we do not sample directly from $\mathcal{N} \left(\log(\lambda_T^{(t)} / \lambda_T^{(c)}), \sqrt{(\lambda_T^{(c)} \Delta t N_T^{(c)})^{-1} + (\lambda_T^{(t)} \Delta t N_T^{(t)})^{-1}} \right)$ as we observed that this does not provide an accurate approximation to the true data-generating process. However, when comparing the power of a frequentist t-test for comparison with Bayesian methods, we assume that the standard error on the log rates ratio is $\sqrt{(\lambda_T^{(c)} \Delta t N_T^{(c)})^{-1} + (\lambda_T^{(t)} \Delta t N_T^{(t)})^{-1}}$ in this case. We assumed $\lambda_T^{(c)} = \lambda_S^{(c)}$, so that $\lambda_T^{(t)} = e^\delta \lambda_S^{(t)}$.

2.2.4 Data generation for recurrent event endpoints

We sampled individual patients' data from a negative binomial distribution, and then estimated the parameters of this distribution from the data.

The negative binomial distribution can be parameterized using its mean μ and the dispersion parameter k . The mean μ is the expected number of failures before achieving k successes. Assuming a normal distribution for the mean, and using the delta method, the standard error of the log event rate ratio is approximated as:

$$\text{SE} \left(\log \left(\frac{\lambda_t}{\lambda_c} \right) \right) \approx \sqrt{\frac{1}{n_t} \cdot \left(\frac{\sqrt{\mu_t + \frac{\mu_t^2}{k}}}{\mu_t} \right)^2 + \frac{1}{n_c} \cdot \left(\frac{\sqrt{\mu_c + \frac{\mu_c^2}{k}}}{\mu_c} \right)^2}$$

2.3 Statistical methods for information borrowing

The choice of statistical methods to be considered for the simulation study is based on an extensive literature review. For each method, we varied the parameters that affect the amount of borrowing. These parameters are summarized in Table S7. The configurations used are summarized in Tables S9 and S10.

2.3.1 Separate analysis and pooling

For each borrowing method, a comparison was made against the power of frequentist analyses that use either full borrowing (pooling) or no borrowing (separate) at the nominal type 1 error rate of 2.5%. The empirical variance is estimated from the sample data, therefore, when the likelihood is Gaussian, the corresponding frequentist test is a t-test. For each method of interest, the power of the t-test was evaluated at different significance levels that depend on the unconditional type 1 error rate of the borrowing method of interest. When the likelihood is given by Figure S1 (Aprepitant case study), we used a test of difference of proportions based on Cohen's h .

For comparison of other operating characteristics and inference metrics, we implemented Bayesian analyses that pool the data or perform a separate analysis.

2.3.2 Conditional Power Prior

As a Bayesian baseline, and to investigate the effect of borrowing without adaptation to prior-data conflict, we started by investigating the effect of fixed borrowing with discounted adult posteriors as priors.

In order to incorporate a fixed amount of information from source studies into the prior for θ_T , Ibrahim and Chen [23] introduced the power prior (also referred to as the Conditional Power Prior (CPP) [24]):

$$\pi(\theta_T | \mathbf{D}_S, \gamma) \propto \mathcal{L}(\theta_T | \mathbf{D}_S)^\gamma \pi_0(\theta_T), \quad (1)$$

where $\gamma \in [0, 1]$, and $\pi_0(\theta_T)$ denotes the so-called "initial" prior distribution for θ_T . The main feature of the method is that the impact of source data on the posterior distribution can be controlled by choosing the value of the power parameter γ , thus providing a simple way of discounting prior information. When $\gamma = 1$, data from the source and target study are pooled, whereas if $\gamma = 0$, data from the source study are discarded. This power parameter allows smoothly changing the analysis from no borrowing to pooling. This method assumes that the parameter of interest θ_T is the same in the source and target studies. In the Normal-Normal model, this is equivalent to inflating the prior variance by a factor $1/\gamma$.

For normal likelihood, we used a custom implementation using the analytical posterior. In the Aprepitant case study, we used a custom implementation that relied on Stan for MCMC inference.

2.3.3 Frequentist test-then-pool

With the frequentist test-then-pool method [1], the idea is to assess the difference between source and target data before deciding whether to pool the data or not. The hypothesis $H_0 : \theta_T = \theta_S$ is tested. If H_0 is rejected, this indicates that the data should not be pooled, and should be analyzed independently. Liu [25] argues that testing the difference between θ_S and θ_T may not be the best approach, and proposed testing an equivalence hypothesis instead, with: $H_0 : |\theta_S - \theta_T| > \lambda$ versus $H_1 : |\theta_S - \theta_T| < \lambda$, where $\lambda > 0$ represents a predetermined equivalence margin. They compute the p -value as the maximum of the p -values for testing two one-sided hypotheses: $H_{0a} : \theta_S - \theta_T > \lambda$ and $H_{0b} : \theta_S - \theta_T < -\lambda$ [26]. Under this approach, a significant p -value implies the rejection of the null hypothesis of non-equivalence.

We investigated both of these approaches using t-tests. Borrowing is determined by the significance level of the equivalence/difference test, and the equivalence margin.

2.3.4 Normalized Power Prior

In the power prior approach, the power prior parameter γ can be treated as a random variable subject to inference by making use of a prior $\pi(\gamma)$ in a hierarchical model. This gives rise to the normalized power prior (NPP, Duan, Ye, Smith, and Smith [27] and Neuenschwander, Branson, and Spiegelhalter [28]), defined as :

$$\pi(\theta_T, \gamma | \mathbf{D}_S) = C(\gamma) \mathcal{L}(\theta_T | \mathbf{D}_S)^\gamma \pi_0(\theta_T) \pi(\gamma), \quad (2)$$

where $C(\gamma)$ is a normalizing constant:

$$C(\gamma) = 1 / \int \mathcal{L}(\theta_T | \mathbf{D}_S)^\gamma \pi_0(\theta_T) d\theta_T. \quad (3)$$

We used a beta prior on the power parameter: $\gamma \sim \text{Beta}(p, q)$, which is a common choice [29, 30]. Analytical derivation for the prior and posterior distributions obtained with a normalized power prior with a normal likelihood, a Beta prior on the power parameter $\gamma \sim \text{Be}(p, q)$, and known standard deviation, can be found in the supplementary material (supplementary section A.2)

Generalizing the Normalized Power Prior to borrow treatment effect in the Aprepitant case study is not straightforward. Therefore, in this case, we assumed a normal likelihood.

2.3.5 Empirical Bayes PP

Gravestock, Held, and COMBACTE-Net consortium [29] proposed an empirical Bayes adaptation of the Normalized Power Prior. The authors derive an analytical posterior for the empirical power prior in the case of a normal likelihood and a beta prior on γ :

$$\hat{\delta} = \frac{\sigma_{\theta_S}^2}{\max \left\{ (\hat{\theta}_T - \hat{\theta}_S)^2, \sigma_{\theta_T}^2 + \sigma_{\theta_S}^2 \right\} - \sigma_{\theta_T}^2}, \quad (4)$$

where the max is required to restrict $\hat{\delta} \leq 1$. Under the same prior and the same likelihood, the empirical Bayes posterior distribution is given by:

$$p(\theta_T | \hat{\theta}_T, \hat{\theta}_S, \delta = \hat{\delta}) \propto \begin{cases} \mathcal{N}(\theta_T | \hat{\theta}_T, \sigma_{\theta_T}^2) \times \mathcal{N}(\theta_T | \hat{\theta}_S, (\hat{\theta}_T - \hat{\theta}_S)^2 - \sigma_{\theta_T}^2) & \text{if } (\hat{\theta}_S - \hat{\theta}_T)^2 > \sigma_{\theta_T}^2 + \sigma_{\theta_S}^2 \\ \mathcal{N}(\theta_T | \hat{\theta}_T, \sigma_{\theta_T}^2) \times \mathcal{N}(\theta_T | \hat{\theta}_S, \sigma_{\theta_S}^2) & \text{otherwise.} \end{cases} \quad (5)$$

2.3.6 P-value based power prior

In a generalization of the test-then-pool approach, Liu [25] proposed a method for selecting the power parameter γ in the Conditional Power Prior based on the p -value of an equivalence test between the source and target data. The function used to determine γ is:

$$\gamma = \exp \left[\frac{k}{1-p} \ln(1-p) \right], \quad (6)$$

where k is a shape parameter that must be specified. More source data is borrowed when the p -value is close to 0 (i.e., the non-equivalence null hypothesis is strongly rejected), and larger values of k imply that more discounting will be applied to the source data for a given p -value. This method can be viewed as an extension of the test-then-pool approach, with the power parameter smoothly adjusting the amount of borrowing from no borrowing to pooling. Again, we used t-tests to compare the source and target studies. In the Aprepitant case study, for all test-then-pool variants (including the p -value-based power prior), we performed a t-test to compute the p -value, then analyzed the data assuming the model structure in Figure S1.

2.3.7 Commensurate Power Prior

The commensurate power prior is given by [31]:

$$\pi(\theta_T, \gamma, \tau | \mathbf{D}_S) = \int \pi(\theta_T | \theta_S, \tau) \frac{\mathcal{L}(\theta_S | \mathbf{D}_S)^\gamma \pi_0(\theta_S)}{\int \mathcal{L}(\theta_S | \mathbf{D}_S)^\gamma \pi_0(\theta_S) d\theta_S} d\theta_S \times p(\gamma | \tau) p(\tau) \quad (7)$$

where $\pi_0(\theta_S)$ is an initial prior for θ_S . Hobbs, Carlin, Mandrekar, and Sargent [31] chose the following distributions:

$$\theta_T | \theta_S, \tau \sim \mathcal{N}\left(\theta_S, \frac{1}{\tau}\right), \text{ and } \gamma | \tau \sim \text{Beta}(g(\tau), 1),$$

where $g(\tau)$ is a positive function of τ that is small for τ closed to zero and large for large values of τ . When the evidence for commensurability is weak, τ is forced toward zero, increasing the variance of the commensurate prior for θ_T . So the amount of borrowing can be adapted in two ways: through the power prior parameter, or through the commensurability parameter.

Hobbs, Carlin, Mandrekar, and Sargent [31] considered the case of Gaussian likelihoods. They chose $g(\log(\tau)) = \max(\log(\tau), 1)$ and put a flat tails Cauchy(0, 30) prior on $\log(\tau)$.

We implemented the commensurate power prior for a variety of priors on the heterogeneity parameter in Stan. However, preliminary tests showed that a Cauchy prior on $\log(\text{heterogeneity})$ could lead to divergence issues. Reducing the scale parameter from 30 to 10 led to relatively similar priors with less divergences. Generalizing the Normalized Power Prior to borrow treatment effect in the Aprepitant case study is not straightforward. Therefore, in this case, we assumed a normal likelihood.

2.3.8 Robust Mixture Prior

Schmidli, Gsteiger, Roychoudhury, O'Hagan, Spiegelhalter, and Neuenschwander [32], based on earlier work by Greenhouse and Wasserman [33], proposed the use of a mixture prior to adapt the amount of borrowing while making the analysis more robust to prior-data conflict:

$$\begin{aligned} \pi(\theta_T | \mathbf{D}_S = d_S) &= w\pi(\theta_T | M_{\text{source}}, \mathbf{D}_S = d_S) \\ &+ (1 - w)\pi(\theta_T | M_{\text{weak}}, \mathbf{D}_S = d_S), \end{aligned} \quad (8)$$

where M_{source} is a model corresponding to either consistency, subject-level exchangeability, or study-level exchangeability. The weight w corresponds to $\Pr(M_{\text{source}} | \mathbf{D}_S)$, the prior belief corresponding to this model. By contrast, M_{weak} is an alternative model corresponding to unrelated treatment effects in the source and target studies. Each component in the mixture corresponds to a different assumption about the relationship between studies: $\pi(\theta_T | M_{\text{source}}, \mathbf{D}_S)$ corresponds to an informative component based on the assumption that studies are related, whereas $\pi(\theta_T | M_{\text{weak}}, \mathbf{D}_S)$ is typically a vague component. The posterior distribution from the source study was used as the informative component $\pi(\theta_T | M_{\text{source}}, \mathbf{D}_S)$.

The posterior distribution of the target study treatment effect θ_T is a weighted average of the posterior distributions under each model, weighted by their respective posterior model probabilities:

$$\begin{aligned} \pi(\theta_T | \mathbf{D}_T = d_T, \mathbf{D}_S = d_S) &= \tilde{w}\pi(\theta_T | M_{\text{source}}, \mathbf{D}_T = d_T, \mathbf{D}_S = d_S) \\ &+ (1 - \tilde{w})\pi(\theta_T | M_{\text{weak}}, \mathbf{D}_T = d_T, \mathbf{D}_S = d_S), \end{aligned} \quad (9)$$

where the updated weight \tilde{w} corresponds to the posterior $\Pr(M_{\text{source}} | \mathbf{D}_T = d_T, \mathbf{D}_S = d_S)$.

So the mixture introduces robustness by allowing the vague prior to dominate if the heterogeneity between source and target trials is large compared to within-trial variance.

As recommended by Schmidli, Gsteiger, Roychoudhury, O'Hagan, Spiegelhalter, and Neuenschwander [32], we selected the variance of the vague component so that it corresponds to a unit-information prior. More precisely, the variance of the vague component is such that it corresponds to the information brought by one subject per arm in the target study. In the case of a normal likelihood, we used the RBeST package. In the Aprepitant case, we relied on a custom implementation using Stan.

2.3.9 Adaptation of existing methods to the settings of interest

Normal likelihood When a normal likelihood is assumed, adapting methods developed to borrow the control arm only to borrow the treatment effect is straightforward. Indeed, we only had to define a prior on the treatment effect instead of the control arm summary measure and to use as likelihood $\mathcal{N}(\hat{\theta}_T | \theta_T, \sigma_{\theta_T}^2)$ instead of $\mathcal{N}(\hat{p}_T^{(t)} | p_T^{(t)}, \sigma_{p_T^{(t)}}^2)$.

Binomial likelihood Adapting methods that borrow the control arm with a binomial likelihood to borrow the treatment effect, with the model structure in Figure S1, is far from straightforward. In these cases, as described in 2.3, we sometimes did not adapt the method and used a normal likelihood instead.

2.4 Analysis of the target trial

2.4.1 Decision criterion

We considered a one-sided null hypothesis $\theta_T \leq \theta_0$ for all case studies except for the Teriflunomide and the Mepolizumab case studies, for which the null hypothesis was $\theta_T \geq \theta_0$. For all scenarios considered, we chose $\theta_0 = 0$.

We denote Θ_0 the null hypothesis space. Given observed data d_S and d_T in the source and target study respectively, it was concluded that $\theta_T \notin \Theta_0$ if the posterior probability $\Pr(\theta_T \notin \Theta_0 | \mathbf{D}_T = d_T, \mathbf{D}_S = d_S) > \eta$, with $\eta = 0.975$. This critical value η is chosen as it is equivalent to requiring the lower limit of the 95% posterior credible interval calculated with the equal-tail method (i.e. with limits corresponding to the quantiles 2.5% and 97.5% of the posterior distribution) for the treatment effect to be outside Θ_0 .

2.4.2 Likelihood

For all case studies except the Aprepitant case study, we assumed that the summary measure of the target study is normally distributed. Therefore, in these cases, $p(\hat{\theta}_T | \theta_T, \sigma_{\theta_T}^2) = \mathcal{N}(\hat{\theta}_T | \theta_T, \sigma_{\theta_T}^2)$, where $\sigma_{\theta_T}^2$ is the standard error on the target treatment effect, which, as explained above, is assumed known and estimated based on the target data sample.

For binary endpoints, we included one case study in which the summary measure was the log odds ratio, modeled on the log scale using a normal distribution (Belimumab, see 2.1.1), and one case (Aprepitant, see 2.1.1) in which, by contrast, the source data consists of $N_S^{(c)}$ (resp. $N_S^{(t)}$) Bernoulli trials with $y_S^{(c)}$ (resp. $y_S^{(t)}$) successes in the control arm (resp. the treatment arm), that is :

$$\begin{aligned} y_T^{(c)} | p_T^{(c)} &\sim \text{Bin}(p_T^{(c)}, N_T) \\ y_T^{(t)} | p_T^{(t)} &\sim \text{Bin}(p_T^{(t)}, N_T^{(t)}) \end{aligned} \quad (10)$$

The corresponding model structure is described in Figure S1.

The likelihood $\mathcal{L}(\theta_T | \mathbf{D}_T)$ is therefore :

$$\begin{aligned} p(\mathbf{D}_T | \theta_T) &= \int_{p_T^{(c)}=0}^1 \int_{p_T^{(t)}=\max(\theta_T, 0)}^{\min(1+\theta_T, 1)} p(\mathbf{D}_T | \theta_T, p_T^{(t)}, p_T^{(c)}) p(p_T^{(t)}, p_T^{(c)} | \theta_T) dp_T^{(t)} dp_T^{(c)} \\ &= \int_0^1 p(\mathbf{D}_T | p_T^{(t)} = \theta_T + p_T^{(c)}, p_T^{(c)}) p(p_T^{(c)}) dp_T^{(c)} \\ &= \int_0^1 \text{Bin}(y_T^{(c)} | p_T^{(c)}, N_T^{(c)}) \text{Bin}(y_T^{(t)} | \theta_T + p_T^{(c)}, N_T^{(t)}) p(p_T^{(c)}) dp_T^{(c)} \end{aligned} \quad (11)$$

We put a uniform prior on $p_T^{(c)}$.

For all case studies, we considered, for simplicity and because this is the most standard setting, that the source and target data likelihoods belong to the same family of distributions.

When assuming a Gaussian likelihood, we considered that the standard error of the summary measure in the target population is known, and we set the standard deviation to the sample standard deviation in the target study, as is often done in meta-analytic approaches and in Bayesian borrowing [34, 20]. However, in practice, the variance of the individual outcome may be substantially larger in the target study. For example, pediatric populations tend to be less homogeneous compared to adults because, for instance, of change in weight with age, organ maturation, and body composition differences [35]. Therefore, we included an additional simulation scenario for the case studies with continuous endpoints (Botox and Dapagliflozin, see section 2.1.1) where the simulated variance in the pediatric data is twice as large as the variance observed in adults.

2.4.3 Prior on the source study treatment effect

When multiple source studies were selected for a given target study, for simplicity, we aggregated their results by simply pooling them. This is the case for the Belimumab and Teriflunomide studies, where adults data come from two studies with identical designs.

Even if the source data are kept fixed, several Bayesian borrowing methods need an initial prior $\pi_0(\theta_S)$ (i.e. prior before extrapolation) to be specified. This is the case, for example, with the family of power priors. For normally distributed treatment effect, we put a vague initial prior $\mathcal{N}(0, 1000)$ on the treatment effect in the source and target studies, except for the Normalized Power Prior [27] and the Empirical Bayes Power Prior [29], for which we relied on existing implementations assuming flat initial priors. When the likelihood was defined on the rates in each arm (in the Aprepitant case study), we used uniform priors on the control rate, $p_c \sim \mathcal{U}(-1, 1)$, and a uniform prior on the treatment effect, $\theta_T | p_c \sim \mathcal{U}(-p_c, 1 - p_c)$.

3 Operating characteristics

3.1 Frequentist operating characteristics

For each method and each scenario, we evaluated the probability of study success, the mean squared error (MSE), bias, precision (measured as the half-width of the 95% Credible Interval), and the coverage probability of the 95% Credible Interval.

The estimated type 1 error rate of the test with borrowing α_B , and the estimated power for $\theta_T > \theta_0$ with borrowing $1 - \beta_B(\theta_T)$ are obtained using the following Monte Carlo approximation :

$$\begin{aligned}\alpha_B &= \frac{1}{N_{\text{sims}}} \sum_{i=1}^{N_{\text{sims}}} \varphi_B(d_T^{(i)} | d_S), d_T^{(i)} \sim p(\mathbf{D}_T | \theta_T = \theta_0) \\ \beta_B(\theta_T) &= \frac{1}{N_{\text{sims}}} \sum_{i=1}^{N_{\text{sims}}} \varphi_B(d_T^{(i)} | d_S), d_T^{(i)} \sim p(\mathbf{D}_T | \theta_T)\end{aligned}\tag{12}$$

where N_{sims} is the number of samples drawn from $p(\mathbf{D}_T | \theta_T)$, and $\varphi_B(d_T^{(i)} | d_S)$ is an indicator of meeting the success criterion with borrowing for dataset $d_T^{(i)}$.

To allow for a fair comparison of the power of the test with and without borrowing, we followed the approach described in Kopp-Schneider, Wiesenfarth, Held, and Calderazzo [36] : we evaluated the TIE rate of the test with borrowing, α_B , and compare the power with and without borrowing ($1 - \beta_B(\theta_T)$ and $1 - \beta(\theta_T)$ respectively) at a TIE of α_B . The test without borrowing was a t-test.

Note that we cannot, in general, determine the power of the t-test analytically, as this would imply differing hypotheses between the separate analysis and the Bayesian methods. To see this, consider that when analytically determining the power of the t-test, we would implicitly assume a χ^2 distribution for the variance. In the Mepolizumab, Teriflunomide and Belimumab case studies, we generated data samples according to some data-generating process, and then assumed a Gaussian likelihood with a known standard deviation for the analysis. The empirical variance does not, in these cases, follow a χ^2 distribution, and the simulation-based estimation of the power does not make this assumption. Therefore, in the Belimumab and Mepolizumab case studies, we determined the frequentist power using simulation. Because of computation time constraints, we did not conduct this analysis in the Teriflunomide case study. This highlights a key requirement when comparing Bayesian and frequentist methods: one must make sure that the comparison between a Bayesian borrowing method and a frequentist test is not impeded by assumptions derived from asymptotic results. A simple way to check this is to compare the frequentist method to a Bayesian method without extrapolation.

For each operating characteristic estimate, we reported the uncertainty due to the finite number of simulations through the 95% Monte Carlo Confidence Intervals. These confidence intervals were estimated using nonparametric bootstrap for metrics other than coverage and probability of success, for which we know the true underlying distribution.

3.2 Prior Effective Sample Size

The amount of borrowing is most easily measured using the concept of prior effective sample size (ESS). Prior ESS corresponds to the number of pseudo-observations required to update a vague conjugate prior to the prior of interest (viewed as the posterior from previous analysis). It is a measure of the informativeness of the prior distribution in terms of number of samples. For instance, in a beta-binomial model, the parameters

of the $Beta(a, b)$ prior can be interpreted as the posterior obtained after observing a successes and b failures, starting from a vague Beta prior (with a and b arbitrarily small). Similarly, a normal prior with variance σ^2/n corresponds to a prior ESS of n , starting from a normal prior with variance σ^2 . However, the prior ESS is not clearly defined for non-conjugate priors. We used several prior ESS measures: the moment-based prior ESS, the precision-based prior ESS, and the ELIR prior ESS.

Moments-based prior ESS We approximated the posterior distribution of the treatment effect using a Gaussian mixture approximation: First, we sampled 1000 samples from the posterior distribution, and we approximated the posterior based on these samples using a mixture of normal distributions using RBest [37]. Then, we computed the ESS of the corresponding mixture approximation. In the Aprepitant case study, before approximating the distribution with a mixture, we linearly transformed the samples so that they fit in the $[0, 1]$ range instead of the $[-1, 1]$ range: we transformed each sample x into $(x + 1)/2$. We computed the moment-based ESS of the mixture approximation, following the method used in the RBest package [37] :

1. Compute the moments of the distribution of interest.
2. Define a distribution from a family for which computing the ESS is trivial (such as normal, beta, or gamma) with the same moments.
3. Compute the corresponding ESS, which is an approximation to the ESS of the distribution of interest.

We then computed the prior ESS as the difference between the posterior ESS and the sample size per arm in the target study.

Precision-based prior ESS The precision-based matching method proceeds as the moment-based matching method, but matches the posterior of interest with a distribution from a family for which computing the ESS is trivial (such as normal, beta, or gamma) with the same precision and mean.

ELIR method for prior ESS. Neuenschwander, Weber, Schmidli, and O'Hagan [38] introduced an information-based ESS, the expected local-information-ratio (ELIR), which has the property of being "predictively consistent", meaning that the expected posterior predictive ESS for a sample of size N_T is equal to the sum of the prior ESS and N_T . The ELIR is defined as follows:

$$ELIR = \mathbb{E}_\theta \left[\frac{\mathcal{I}_\pi(\theta)}{\mathcal{I}_1(\theta)} \right] \quad (13)$$

where $\mathcal{I}_1(\theta)$ is the expected Fisher information for one information unit, given by:

$$\mathcal{I}_1(\theta) = -\mathbb{E} \left[\frac{\partial^2 \log \mathcal{L}(\theta | \mathbf{D}_1)}{\partial \theta^2} \middle| \theta \right], \quad (14)$$

and \mathbf{D}_1 denotes a dataset with one subject per arm. We determined the prior ELIR ESS using the RBest package [37].

4 Results

4.1 Impact of borrowing on the probability of success

Impact of the drift on Type I error Type I error inflation, that is, a type 1 error increase above the value α that would be obtained for a Bayesian separate analysis with a critical value $\eta = 1 - \alpha$, is the main concern when using partial extrapolation in the context of clinical trials. We observed type 1 error rate inflation in the vast majority of scenarios, irrespective of the method used and its parameterization. The only cases where inflation was not observed corresponded to the Botox case study when the ratio between the target and source standard deviation was two, with the Conditional Power Prior with $\gamma = 0.25$, and small sample sizes in the target trial ($N_T/2 = 58$ or 39). In the Teriflunomide case, the absence of TIE inflation occurred when the denominator of the source study summary measure was halved. We systematically observed TIE inflation due to borrowing in the Aprepitant, Mepolizumab, and Dapagliflozin case studies.

Figure 1 (left panel) illustrates type 1 error rate inflation across the different methods in the Botox case study.

Power gains at equivalent type 1 error control [39] showed that borrowing information cannot provide more power at an equivalent type 1 error, irrespective of the type 1 error rate, when a Uniformly Most Powerful (UMP) test exists. This implies that the improved power is simply bought at the expense of type 1 error inflation (see Figure S3 for an example of the power curve of the CPP, comparable to the one of the frequentist t-test without borrowing at equivalent TIE α_B).

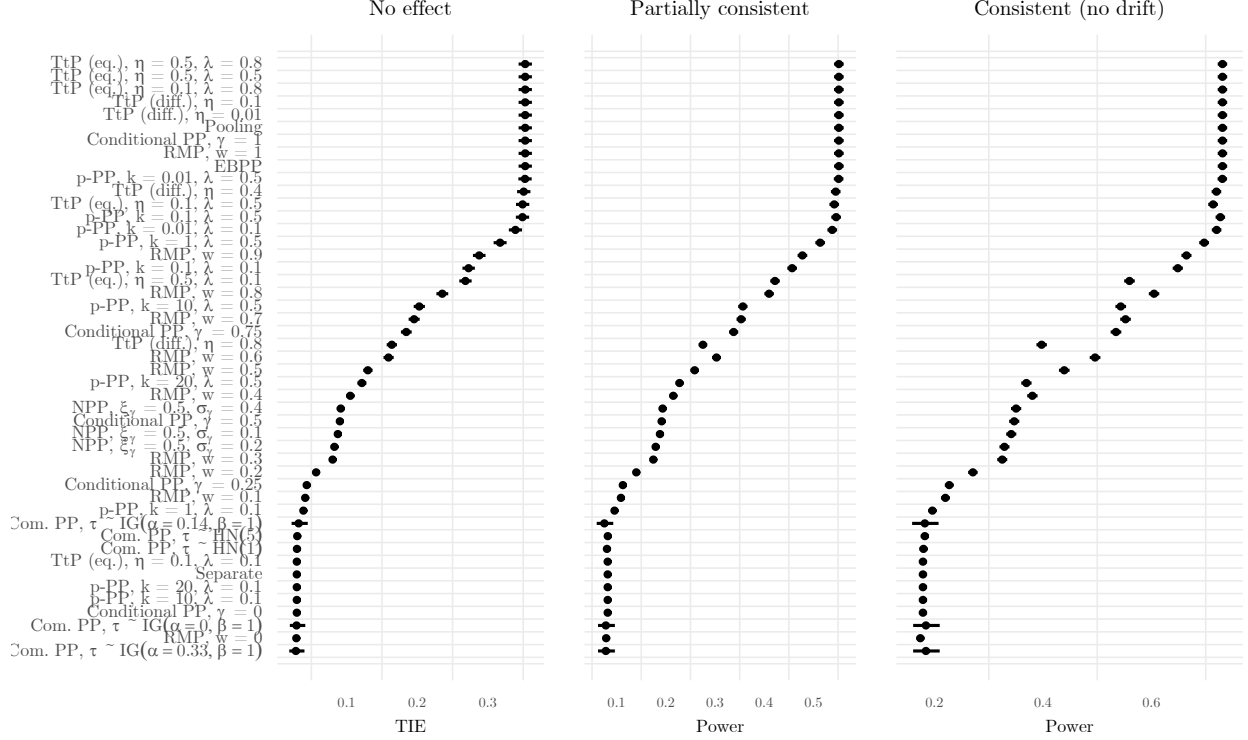


Figure 1: Probability of success across all simulation replicates and associated 95% CI, for the three main treatment effects considered, in the Botox case study with 58 samples per arm in the target trial. The ordering of methods is made with respect to the type 1 error rate (absence of effect, corresponding to a large drift)

Power loss due to borrowing Kopp-Schneider, Wiesenfarth, Held, and Calderazzo [36] reported that, in some "extreme borrowing" cases, Bayesian borrowing methods can lead to non-UMP tests, and therefore to power loss compared to a separate analysis (illustrated in Figure S4).

This phenomenon occurred for all methods, mostly for a very small target study sample size. Moreover, a ratio between the source and target standard deviation of 2 (instead of 1) also increased the sensitivity of methods to this phenomenon.

To get a more precise understanding of which methods incur such power losses, we compared the power of each method as a function of type 1 error (Figure 2). We observed that most methods aligned on a similar power vs type 1 error rate curve. However, the test-then-pool variants tended to show decreased power at equivalent type 1 error rate compared to other methods. Conditional PP consistently emerges as the most robust method, exhibiting the highest success probabilities at equivalent TIE rate.

4.2 Impact of drift on the amount of borrowing.

Comparing the prior ESS to the sample size in the target study is a convenient way of comparing the amount of information borrowed from the source study to the information content of the target study. However, interpretation of the impact of drift on the prior ESS can be difficult when summary measures are, e.g., risk ratios or odds ratios, as the standard deviation in the target study depends on the drift. Similarly, an increase in the standard deviation in the target study compared to the source study would naturally increase the prior ESS. Therefore, we focused our analysis on the Botox and Dapagliflozin case studies (normally distributed endpoints), without change incurred in the standard deviation in the target study. We observed (Figure 3) that, overall, in the range of drift values considered, the adaptiveness of the different methods was quite limited. No method displayed a radical shift in ESS between the consistent and no-effect scenarios. From a practical perspective, one may focus on methods and parameters for which the prior ESS is lower than $N_T/2$, as it may not be acceptable that the source trial provides more information for inference than the target trial.

For very large drift, adaptive borrowing methods discard external information, and their frequentist operating characteristics are therefore equivalent to those of frequentist methods (see e.g. Figure S7).

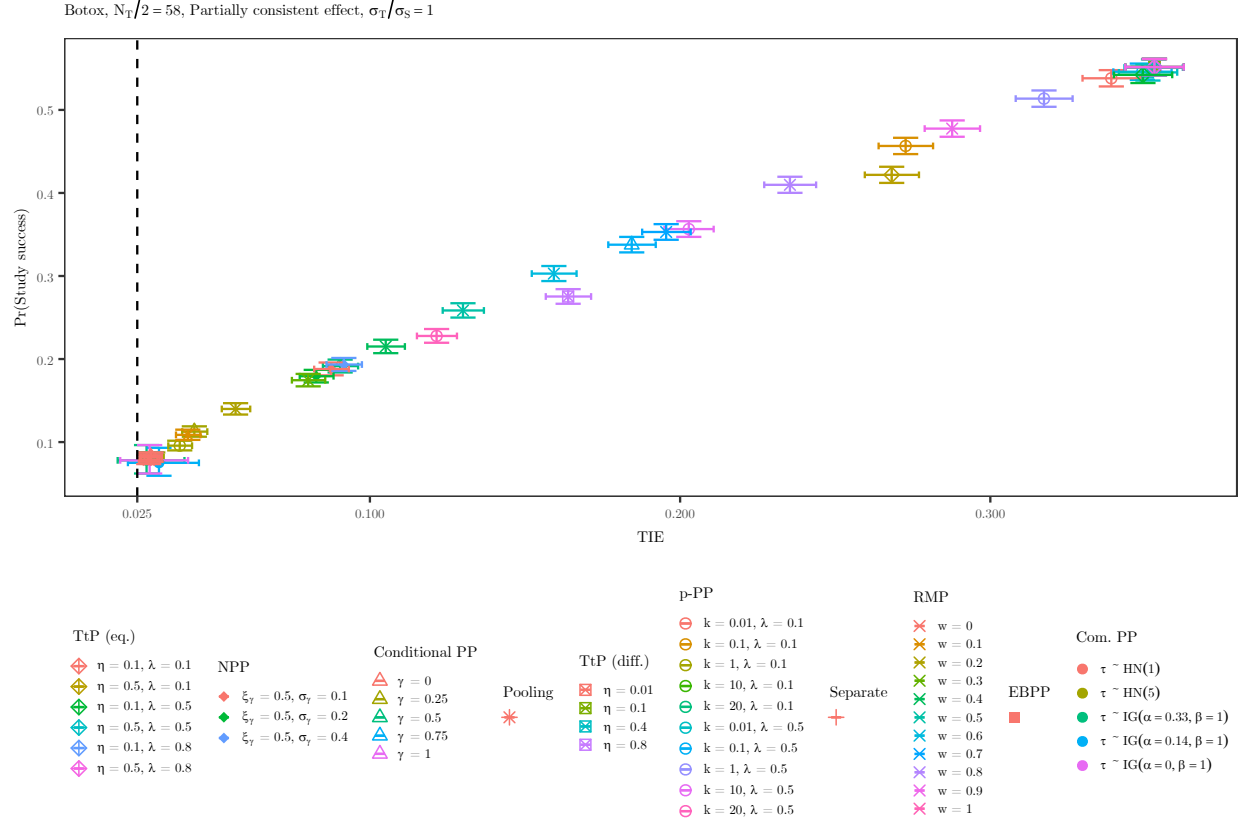


Figure 2: Probability of success as a function of type 1 error rate in the Botox case study with a sample size per arm of 58, across all the methods and parameters. The treatment effect is partially consistent, the target to source standard deviation ratio is 1. Error bars correspond to the 95% Confidence Interval of the Probability of Success and type 1 error rate. Dashed vertical line represents the nominal type 1 error rate of 0.025.

4.3 Impact of borrowing on bias and precision

Bias and precision are the two main components to consider when comparing methods concerning their estimation performance. Here, precision is measured as the half-width of the 95% Credible Interval. It measures the strength of the belief represented by the posterior distribution. The mean-squared error (MSE) directly relates to the tradeoff between precision and bias. Figure 4 compares the MSE of the different methods in the Botox case study for the three main treatment effects considered. In the absence of drift, borrowing reduces MSE. This is explained by the absence of bias, and the reduction of the variance of the posterior distribution (that is, improved precision) due to borrowing (Figure S6). As drift increases, however, bias will also tend to increase (Figure S5), although, for extreme drift values, adaptive borrowing methods discard the source data, hence reducing bias. Moreover, the precision of adaptive borrowing methods decreases (i.e., the half-width of the 95% increases) as the drift in treatment increases. This can be understood by considering the behavior of the prior ESS of adaptive borrowing methods with drift : the prior ESS also decreases similarly when the drift value goes away from zero. This implies that the posterior will be less sharp, hence the wider 95% confidence interval.

Comparison of methods regarding bias, precision and MSE is made difficult by the fact that these operating characteristics largely depend on the parameters chosen for the method. Considering that type 1 error is of main interest from a regulatory perspective, we plotted, for each method/parameters combination, the MSE against the type 1 error rate of the corresponding method (Figure 5). This provides a measure of the accuracy of the estimation for a given type 1 error rate inflation. We observed that, across the different case studies and scenarios, the conditional power prior and the RMP seemed to perform better than other methods regarding MSE at equivalent type 1 error rate, although this was not a systematic pattern. We

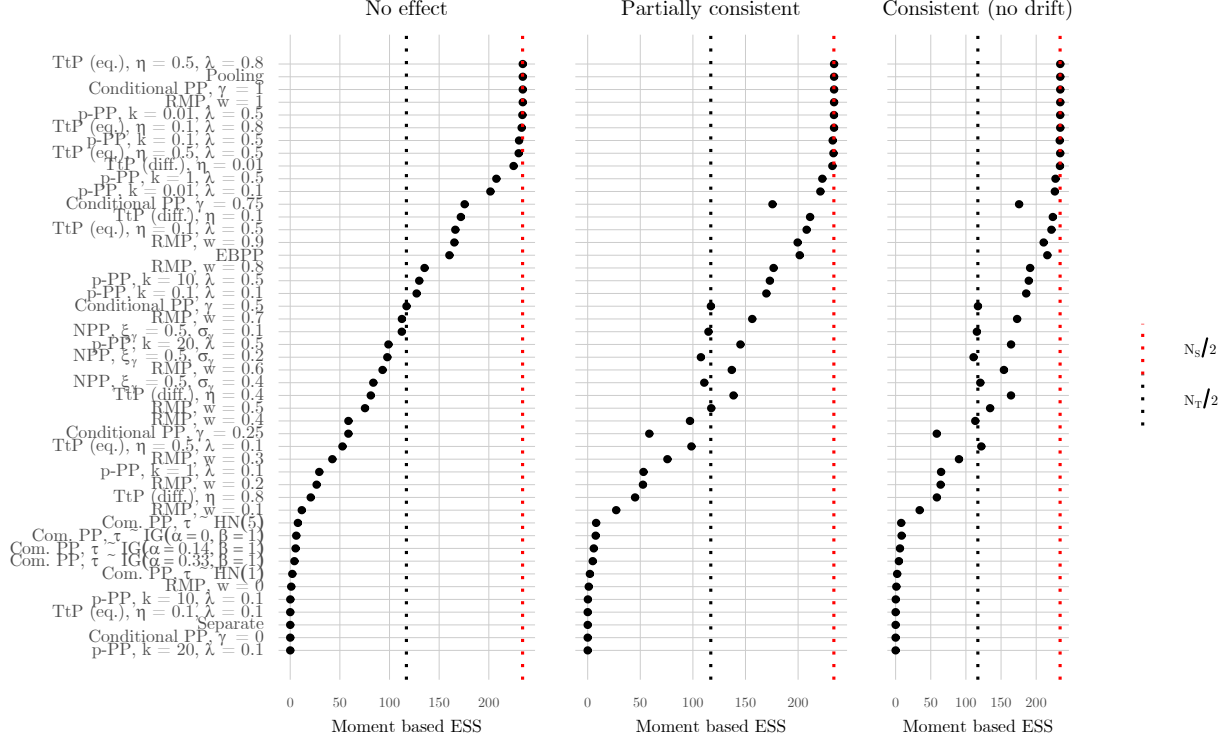


Figure 3: Moment-based ESS across methods and for the three main treatment effects considered in the Botox case study. The red dashed line corresponds to an ESS equal to the source study sample size per arm, and the black dashed line corresponds to the target study sample size per arm.

observed that the test-then-pool variants and the p-value-based power prior tended to incur much larger MSE than other methods at similar type 1 error rates.

4.4 Impact of borrowing on the coverage probability of the 95% Credible Interval.

The coverage probability of the 95% Credible Interval is a measure of the calibration of the uncertainty of a Bayesian method. It is key to consider, as it provides a measure of the trust we can put in interpretations of credible intervals. In the absence of drift, methods that systematically pool the data lead to a coverage probability larger than 0.95, but the coverage largely decreases as the drift increases (Figure S9). We noticed that in the presence of drift, increased sample size improved the coverage probability.

We observed, when plotting the coverage as a function of type 1 error (Figure S10), that the p-value-based power prior and the test-then-pool variants performed worse than other methods at similar type 1 error rate. Overall, the conditional power prior seemed to perform better.

4.5 Relationship between prior ESS and frequentist operating characteristics

In reporting the results of the simulation study, we focused on a comparison of operating characteristics at similar type 1 error. However, given that the magnitude of the prior ESS relative to the target study sample size is a key consideration when selecting a prior, one may wonder whether the results of comparisons at similar prior ESS would be in agreement with those made at equivalent TIE. Interestingly, we noticed that this was the case overall, yet with better performance of the Conditional Power Prior and RMP relative to other methods at equivalent prior ESS (Figure S8).

Figure 4: Comparison of the Mean Squared Error (MSE) of the different methods and associated 95% CI, for the three main treatment effects considered, in the Botox case study with 117 samples per arm in the target trial.

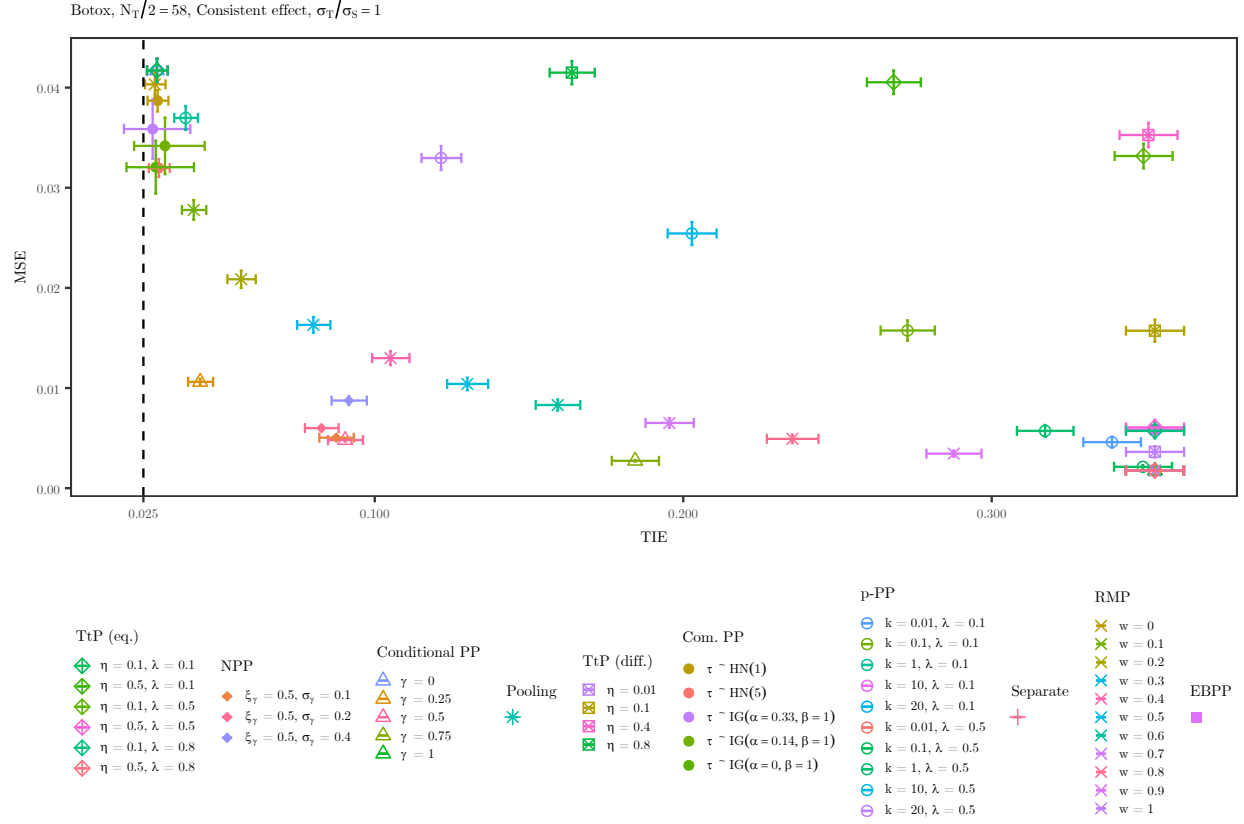


Figure 5: MSE as a function of type 1 error rate in the Botox case study with a sample size per arm of 58, across all the methods and parameters. The treatment effect is consistent, the target to source standard deviation ratio is 1. Error bars correspond to the 95% Confidence Interval of the MSE. Dashed vertical line represents the nominal type 1 error rate of 0.025.

5 Discussion

Despite the growing interest in the use of partial extrapolation methods in the design and analysis of clinical trials to overcome reduced sample size problems, their use for treatment effect borrowing, e.g. in rare diseases or pediatrics, remains limited [40]. One of the reasons is that analytically controlling the type I error rate of a design making use of dynamic borrowing is usually intractable, in particular when using non-conjugate models (see however Nikolakopoulos, Tweel, and Roes [41] and Calderazzo, Wiesenfarth, and Kopp-Schneider [42]). This can be problematic as regulatory agencies prefer statistical methods that do so [43].

Because of the uncertainty associated with the performance of a given method, it is usually recommended to run extensive simulation studies tailored to the specific problem at hand and to the available source data. This is important both for comparing existing methods, selecting a prior and its hyperparameters (e.g., between-trials variance, power parameter, mixture weights), and estimating the sample size that can be spared. However, statistical recommendations are lacking for simulation studies specifically tailored to the problem of treatment-effect borrowing.

In this paper, we report a large-scale simulation study inspired by real use cases to compare existing methods in a unified simulation-based assessment framework. We explored a wide diversity of scenarios by varying the sample size of the clinical trial in the target population, the magnitude of the treatment effect, the variance in the target study, the type of endpoint, as well as the parameters needed to specify the models.

5.1 Probability of success of borrowing methods

The simulation study results show that borrowing treatment effects almost systematically leads to an increased type 1 error rate, to an extent that strongly depends on methods and method parameters. This is in agreement with previous literature [44].

It is therefore difficult to control the type 1 error of adaptive borrowing methods, although some methods such as the PDCCPP [41] have been proposed that do so (see also Calderazzo and Kopp-Schneider [45]). Overall, static borrowing methods, in combination with calibration, provide a straightforward way to control type 1 error to a pre-specified value.

Bayesian borrowing methods are sometimes motivated by potential power gains compared to frequentist methods, with some authors suggesting, in the case of historical control borrowing, that this can be achieved at equivalent or lower type 1 error rate Viele et al. [1] and Yang, Zhao, Nie, Vallejo, and Yuan [46]. However, Kopp-Schneider, Calderazzo, and Wiesenfarth [39] (preceded by Psioda and Ibrahim [47] in the Gaussian case) showed that, in terms of power gain, "approaches adaptively discounting prior information do not offer any advantage over a fixed amount of borrowing, or no borrowing at all", when a Uniformly Most Powerful (UMP) test exists, which is the case in most settings encountered in confirmatory trials.

Moreover, Kopp-Schneider, Wiesenfarth, Held, and Calderazzo [36] shows that, in some "extreme borrowing" cases, Bayesian borrowing methods lead to non-UMP tests, so that their power at equivalent type 1 error rate is lower compared to frequentist methods. We observed this tendency, in particular, with test-then-pool variants in case of consistent treatment effect.

5.2 Performance of partial extrapolation methods

The model parameters modulating information borrowing allow for controlling the amount of borrowing and the response of the operating characteristics to drift. For methods such as the RMP, the Conditional Power Prior, the Commensurate Power Prior, and the test-then-pool variants, it is possible to adjust the borrowing parameters in the spectrum that goes from no borrowing to pooling. The NPP has a different behavior, as it never fully pools the source and target study data.

Due to the dependency of methods' behavior on their parameters, and the absence of direct mapping between the parameters of different methods, is difficult to directly compare them. One approach may be to consider an operating characteristic of main interest, for example, the type 1 error rate, and to compare methods anchored on this operating characteristic (e.g. a target TIE rate of 0.1). This requires calibrating the borrowing parameters to match the target value. We did not consider this in our simulation study design due to the implied computational burden, but future work could consider the following approach:

1. Define the operating characteristic for which we need equivalent value across methods to compare them, and define its target value.
2. In a given scenario, calibrate the method's parameters to reach the target value for the OC of interest.
 - Define the range of parameters considered
 - Define a small number of simulation replicates used only for calibration

- Use an optimization algorithm to find the parameters values for which the method matches the target OC.

3. Run a simulation study with the calibrated parameters with a large number of replicates.

However, this approach implies a nested simulation, and can therefore be computationally highly expensive. However, it is practically feasible if the number of scenarios and methods to consider is small. An advantage is that, in addition to allowing a fair comparison between methods, it directly allows anchoring an OC of interest, such as type 1 error rate, to a pre-specified value.

We instead approached the comparison of borrowing methods by considering whether, at a similar type 1 error rate, other characteristics would be more or less improved. Although we were not able to compare methods at exactly the same type 1 error rates, since we included many methods and parameters, it was possible to make meaningful comparisons.

Our results show that methods do not behave equally for a given increase in type 1 error rate. In particular, we observed that the p-value-based Power Prior and the test-then-pool variants displayed a larger MSE (worse accuracy) at a similar type 1 error rate compared to other methods, and were less robust to drift when considering MSE. These methods, as well as the EBPP, also showed a strong reduction in uncertainty calibration in case of drift, as measured using the coverage probability of the 95% CrI. These elements provide a strong argument against the use of such methods.

In each case study, it was not possible to identify a method that would systematically perform better compared to others in terms of power gains, estimation accuracy, and coverage. For example, we observed that the RMP with prior weight in the range 0.1 to 0.9 displayed a more robust coverage probability compared to other adaptive borrowing methods, but similar to the Conditional Power Prior.

A surprising result is the overall good performance of the Conditional Power Prior—a fixed borrowing method—compared to adaptive borrowing method. Over all scenarios and case studies, the Conditional Power Prior was among the best-performing methods when comparing at equivalent type 1 error rate, performing better than the RMP in terms of MSE in many cases. This may seem counterintuitive, as one may expect adaptive borrowing methods to incur lower MSE in the presence of drift. However, one has to consider the fact that, when comparing methods at equivalent type 1 error rate, comparison is performed after adaptation, and therefore at similar prior ESS.

Beyond the methods' performance in the simulation study, it is important to consider that different may have very different underlying assumptions. Some methods, such as the Conditional Power Prior, assume the treatment effect in both source and target populations in the same, whereas others include separate parameters for both and rely on the assumption of exchangeability between the source and target study.

Code availability

The R code developed in this study is available as a GitHub repository at <https://github.com/quinten-health-os/BayesianExtrapolationSimulation>. It can be used to run and analyze simulation studies and for analyzing data using partial extrapolation. The exact version that was used for running the simulation study is v0.0.2, whereas the version that was used for the analysis of the results, results quality checks, and for producing tables and figures is v0.0.3.

The code was reviewed by a team member who did not directly participate in the implementation. Statistical accuracy of the results was validated based on manual checks, involving a comparison of the figures produced with relevant published figures.

Funding

This project was funded through the reopening of competition no. 02 under framework contract following procurement procedure EMA/2020/46/TDA (Lot 3).

Acknowledgements

We thank EMA experts Dr Juan José Abéllan Andrés and Dr Andrew Thompson for guidance and help in the planning, execution and reporting of this study. We thank Marie Génin for project management, and Daniel Lee for help with the use of Stan.

This work was granted access to the HPC/AI resources of the French National Computer Center for Higher Education (CINES) under the allocation 2024-AD010315186 made by the Grand Equipement National de Calcul Intensif (GENCI).

References

- [1] Viele, K. et al. "Use of historical control data for assessing treatment effects in clinical trials." *Pharmaceutical Statistics* 13.1 (2014), 41–54.
- [2] Viele, K., Mundy, L. M., Noble, R. B., Li, G., Broglio, K., and Wetherington, J. D. "Phase 3 adaptive trial design options in treatment of complicated urinary tract infection". *Pharmaceutical Statistics* 17.6 (2018), 811–822.
- [3] Lim, J. et al. "Reducing Patient Burden in Clinical Trials Through the Use of Historical Controls: Appropriate Selection of Historical Data to Minimize Risk of Bias". *Therapeutic Innovation & Regulatory Science* 54.4 (2020), 850–860.
- [4] Best, N., Ajimi, M., Neuenschwander, B., Saint-Hilary, G., and Wandel, S. *Beyond the classical type I error: Bayesian metrics for Bayesian designs using informative priors*. 2023.
- [5] Wang, Y., Travis, J., and Gajewski, B. "Bayesian adaptive design for pediatric clinical trials incorporating a community of prior beliefs". *BMC medical research methodology* 22.1 (2022), 118.
- [6] Shehadeh, N. et al. "Dapagliflozin or Saxagliptin in Pediatric Type 2 Diabetes". *NEJM Evidence* (2023).
- [7] Bailey, C. J., Gross, J. L., Pieters, A., Bastien, A., and List, J. F. "Effect of dapagliflozin in patients with type 2 diabetes who have inadequate glycaemic control with metformin: a randomised, double-blind, placebo-controlled trial". *Lancet (London, England)* 375.9733 (2010), 2223–2233.
- [8] Bailey, C. J., Gross, J. L., Hennicken, D., Iqbal, N., Mansfield, T. A., and List, J. F. "Dapagliflozin add-on to metformin in type 2 diabetes inadequately controlled with metformin: a randomized, double-blind, placebo-controlled 102-week trial". *BMC medicine* 11 (2013), 43.
- [9] Psioda, M. A. and Xue, X. "A Bayesian Adaptive Two-stage Design for Pediatric Clinical Trials". *Journal of Biopharmaceutical Statistics* 30.6 (2020), 1091–1108.
- [10] Brunner, H. I. et al. "Safety and efficacy of intravenous belimumab in children with systemic lupus erythematosus: results from a randomised, placebo-controlled trial". *Annals of the Rheumatic Diseases* 79.10 (2020), 1340–1348.
- [11] Pottackal, G. et al. "Application of Bayesian Statistics to Support Approval of Intravenous Belimumab in Children with Systemic Lupus Erythematosus in the United States". *Arthritis Rheumatol.* 2019.
- [12] Jin, M., Li, Q., and Kaur, A. "Bayesian Design for Pediatric Clinical Trials with Binary Endpoints When Borrowing Historical Information of Treatment Effect". *Therapeutic Innovation & Regulatory Science* 55.2 (2021), 360–369.
- [13] Diemunsch, P. et al. "Single-dose aprepitant vs ondansetron for the prevention of postoperative nausea and vomiting: a randomized, double-blind phase III trial in patients undergoing open abdominal surgery". *British Journal of Anaesthesia* 99.2 (2007), 202–211.
- [14] Salman, F. T., DiCristina, C., Chain, A., and Afzal, A. S. "Pharmacokinetics and pharmacodynamics of aprepitant for the prevention of postoperative nausea and vomiting in pediatric subjects". *Journal of Pediatric Surgery* 54.7 (2019), 1384–1390.
- [15] Jin, H. and Yin, G. "Unit information prior for adaptive information borrowing from multiple historical datasets". *Statistics in Medicine* 40.25 (2021), 5657–5672.
- [16] Chitnis, T. et al. "Safety and efficacy of teriflunomide in paediatric multiple sclerosis (TERIKIDS): a multicentre, double-blind, phase 3, randomised, placebo-controlled trial". *The Lancet Neurology* 20.12 (2021), 1001–1011.
- [17] Bovis, F., Ponzano, M., Signori, A., Schiavetti, I., Bruzzi, P., and Sormani, M. P. "Reinterpreting Clinical Trials in Children With Multiple Sclerosis Using a Bayesian Approach". *JAMA Neurology* 79.8 (2022), 821.
- [18] O'Connor, P. et al. "Randomized Trial of Oral Teriflunomide for Relapsing Multiple Sclerosis". *New England Journal of Medicine* 365.14 (2011), 1293–1303.
- [19] Confavreux, C. et al. "Oral teriflunomide for patients with relapsing multiple sclerosis (TOWER): a randomised, double-blind, placebo-controlled, phase 3 trial". *The Lancet Neurology* 13.3 (2014), 247–256.
- [20] Best, N., Price, R. G., Pouliquen, I. J., and Keene, O. N. "Assessing efficacy in important subgroups in confirmatory trials: An example using Bayesian dynamic borrowing". *Pharmaceutical Statistics* 20.3 (2021), 551–562.
- [21] Ortega, H. G. et al. "Mepolizumab Treatment in Patients with Severe Eosinophilic Asthma". *New England Journal of Medicine* 371.13 (2014), 1198–1207.

- [22] Keene, O., Best, N., Price, R., and Pouliquen, I. "Use of a novel Bayesian borrowing statistical method to assess efficacy of mepolizumab in adolescents". *Paediatric asthma and allergy*. ERS International Congress 2020 abstracts. European Respiratory Society, 2020, 667.
- [23] Ibrahim, J. G. and Chen, M.-H. "Power prior distributions for regression models". *Statistical Science* 15.1 (2000), 46–60.
- [24] Neelon, B. and O'Malley, A. J. "Bayesian Analysis Using Power Priors with Application to Pediatric Quality of Care". *Journal of biometrics & biostatistics* 2010.1 (2010), 1–9.
- [25] Liu, G. F. "A dynamic power prior for borrowing historical data in noninferiority trials with binary endpoint". *Pharmaceutical Statistics* 17.1 (2018), 61–73.
- [26] Schuirmann, D. J. "A comparison of the Two One-Sided Tests Procedure and the Power Approach for assessing the equivalence of average bioavailability". *Journal of Pharmacokinetics and Biopharmaceutics* 15.6 (1987), 657–680.
- [27] Duan, Y., Ye, K., Smith, E. P., and Smith, E. "Evaluating water quality using power priors to incorporate historical information". *Environmetrics* 17.1 (2006), 95–106.
- [28] Neuenschwander, B., Branson, M., and Spiegelhalter, D. J. "A note on the power prior: A NOTE ON THE POWER PRIOR". *Statistics in Medicine* 28.28 (2009), 3562–3566.
- [29] Gravestock, I., Held, L., and COMBACTE-Net consortium. "Adaptive power priors with empirical Bayes for clinical trials: Adaptive Power Priors with Empirical Bayes for Clinical Trials". *Pharmaceutical Statistics* 16.5 (2017), 349–360.
- [30] Shi, Y., Li, W., and Liu, G. F. "A novel power prior approach for borrowing historical control data in clinical trials". *Statistical Methods in Medical Research* 32.3 (2023), 9622802221146309.
- [31] Hobbs, B. P., Carlin, B. P., Mandrekar, S. J., and Sargent, D. J. "Hierarchical commensurate and power prior models for adaptive incorporation of historical information in clinical trials". *Biometrics* 67.3 (2011), 1047–1056.
- [32] Schmidli, H., Gsteiger, S., Roychoudhury, S., O'Hagan, A., Spiegelhalter, D., and Neuenschwander, B. "Robust meta-analytic-predictive priors in clinical trials with historical control information: Robust Meta-Analytic-Predictive Priors". *Biometrics* 70.4 (2014), 1023–1032.
- [33] Greenhouse, J. B. and Wason, L. "Robust bayesian methods for monitoring clinical trials". *Statistics in Medicine* 14.12 (1995), 1379–1391.
- [34] Weber, K., Hemmings, R., and Koch, A. "How to use prior knowledge and still give new data a chance?". *Pharmaceutical Statistics* 17.4 (2018), 329–341.
- [35] Kern, S. E. "Challenges in conducting clinical trials in children: approaches for improving performance". *Expert Review of Clinical Pharmacology* 2.6 (2009), 609–617.
- [36] Kopp-Schneider, A., Wiesenfarth, M., Held, L., and Calderazzo, S. "Simulating and reporting frequentist operating characteristics of clinical trials that borrow external information". *arXiv* (2023).
- [37] AG, N. P. et al. *RBesT: R Bayesian Evidence Synthesis Tools*. Version 1.6-6. 2023.
- [38] Neuenschwander, B., Weber, S., Schmidli, H., and O'Hagan, A. "Predictively consistent prior effective sample sizes". *Biometrics* 76.2 (2020), 578–587.
- [39] Kopp-Schneider, A., Calderazzo, S., and Wiesenfarth, M. "Power gains by using external information in clinical trials are typically not possible when requiring strict type I error control". *Biometrical Journal. Biometrische Zeitschrift* 62.2 (2020), 361–374.
- [40] Partington, G., Cro, S., Mason, A., Phillips, R., and Cornelius, V. "Design and analysis features used in small population and rare disease trials: A targeted review". *Journal of Clinical Epidemiology* 144 (2022), 93–101.
- [41] Nikolakopoulos, S., Tweel, I. van der, and Roes, K. C. B. "Dynamic borrowing through empirical power priors that control type I error: Dynamic Borrowing with Type I Error Control". *Biometrics* 74.3 (2018), 874–880.
- [42] Calderazzo, S., Wiesenfarth, M., and Kopp-Schneider, A. "A decision-theoretic approach to Bayesian clinical trial design and evaluation of robustness to prior-data conflict". *Biostatistics (Oxford, England)* 23.1 (2022), 328–344.
- [43] Collignon, O. et al. "Adaptive designs in clinical trials: from scientific advice to marketing authorisation to the European Medicine Agency". *Trials* 19.1 (2018), 642.
- [44] Campbell, G. "Bayesian methods in clinical trials with applications to medical devices". *Communications for Statistical Applications and Methods* 24.6 (2017), 561–581.
- [45] Calderazzo, S. and Kopp-Schneider, A. *Robust incorporation of historical information with known type I error rate inflation*. 2022.

- [46] Yang, P., Zhao, Y., Nie, L., Vallejo, J., and Yuan, Y. *SAM: Self-adapting Mixture Prior to Dynamically Borrow Information from Historical Data in Clinical Trials*. 2023.
- [47] Psioda, M. A. and Ibrahim, J. G. "Bayesian clinical trial design using historical data that inform the treatment effect". *Biostatistics (Oxford, England)* 20.3 (2019), 400–415.
- [48] Pawel, S., Aust, F., Held, L., and Wagenmakers, E.-J. "Normalized power priors always discount historical data". *Stat* 12.1 (2023), e591.
- [49] Hoffman, M. D. and Gelman, A. "The No-U-Turn Sampler: Adaptively Setting Path Lengths in Hamiltonian Monte Carlo" (2011).
- [50] Brunner, H. I. et al. "Efficacy and safety of belimumab in paediatric and adult patients with systemic lupus erythematosus: an across-study comparison". *RMD Open* 7.3 (2021), e001747.

Supplementary material

A Supplementary methods

A.1 Definition of the drift ranges

However, with an adaptive borrowing method, the probability of meeting the decision criterion, $\Pr(\text{Study success} | \mathbf{D}_T = \mathbf{d}_T, \mathbf{D}_S = \mathbf{d}_S)$, is expected to reach a maximum at some drift value beyond which source data starts being discarded. For the study of adaptive borrowing methods, it is thus important to select a range of drift wide enough for this discarding phenomenon to be observed.

To determine the range of drift to consider for a given case study, we propose the following rationale when the likelihood is Gaussian: one may consider that if the overlap between the posterior distribution of the treatment effect in the source study $p(\theta_S | \mathbf{y}_S)$ and the target study $p(\theta_T | \mathbf{y}_T)$ is very small, the source study should be discarded. To include this idea in our simulation framework, we analytically determined, for a given value of $\theta_T = \hat{\theta}_S + \delta$, the Hellinger distance between $\mathcal{N}(\hat{\theta}_S, \sigma_{\theta_S}^2)$, where σ_{θ_S} is the standard error on θ_S , and $\mathcal{N}(\hat{\theta}_S + \delta, \sigma_{\theta_T}^2)$, where σ_{θ_T} is the standard error on θ_T derived from the observed target study data alone.

We determined the value of the negative drift for which the Hellinger distance reaches 0.9, and used this as the lower boundary of the drift ranges considered. Beyond such an extreme value for the observed drift, borrowing from source data can be considered futile. Note that, for simplicity, we used the same drift range for all scenarios in a given case study, irrespective of later changes introduced in the denominator of source ratio-like summary measures or target study sampling standard deviation.

Note that in cases where the posterior predictive $p(\bar{y}_T | \theta_T, \sigma_{\theta_T}^2)$ is very wide, it may not be guaranteed that the range $[\theta_0 - \hat{\theta}_S, 0]$ is included within the drift range obtained with the above method (noted \mathcal{R}). Although this case may happen in very rare cases given the quite conservative threshold of 0.9 considered, we used the range $\mathcal{R} \cup [\theta_0 - \hat{\theta}_S, 0]$ for the drift in practice. We observed that $[\theta_0 - \hat{\theta}_S, 0] \subset \mathcal{R}$ in all case studies considered.

When the treatment effect is a difference of rates, $\theta_T = p_T^{(t)} - p_T^{(c)}$, where $p_T^{(a)}$ is the response rate in arm a of the target trial, θ_T spans the range $[-1, 1]$. Therefore the drift spans the interval $[-1 - \hat{\theta}_S, 1 - \hat{\theta}_S]$. Moreover, we need to ensure that $p_T^{(t)}$ and $p_T^{(c)}$ are within $[0, 1]$. Since we assume $p_T^{(c)} = \hat{p}_S^{(c)}$, we have:

$$p_T^{(t)} = \theta_T + p_T^{(c)} = \delta + \hat{\theta}_S + \hat{p}_S^{(c)} = \delta + \hat{p}_S^{(t)} \quad \text{This implies the following constraint: } -\hat{p}_S^{(t)} \leq \delta \leq 1 - \hat{p}_S^{(t)}.$$

By combining these two constraints, the drift interval is $\mathcal{R} = [\max(-1 - \hat{\theta}_S, -\hat{p}_S^{(t)}), \min(1 - \hat{\theta}_S, 1 - \hat{p}_S^{(t)})]$.

The corresponding drift ranges considered for each case study are listed in Supplementary Table S2. We considered evenly spaced values in the range of drift. Note that, for computational cost reasons, we did not use the same number of drift values for each method and each case study.

A.2 Normalized Power Prior

Pawel, Aust, Held, and Wagenmakers [48] or in appendix A of Gravestock, Held, and COMBACTE-Net consortium [29]. In this setting, the normalized power prior is:

$$\pi(\theta_T, \gamma | \mathbf{D}_S) = \frac{\mathcal{L}(\mathbf{D}_S | \theta_T)^\gamma \pi(\gamma)}{\int_{-\infty}^{+\infty} \mathcal{L}(\mathbf{D}_S | \theta'_T)^\gamma d\theta'_T} = \mathcal{N}(\theta_T | \hat{\theta}_S, \sigma_{\theta_S}^2 / \gamma) \text{Be}(\gamma | p, q)$$

The marginal prior on θ_T is :

$$\begin{aligned} \pi(\theta_T | \mathbf{D}_S) &= \int_0^1 \mathcal{N}(\theta_T | \hat{\theta}_S, \sigma_{\theta_S}^2 / \gamma) \text{Be}(\gamma | p, q) d\gamma \\ &\propto \text{M}\left(\frac{1}{2} + p, \frac{1}{2} + p + q, -\frac{(\hat{\theta}_S - \theta_T)^2}{2\sigma_{\theta_S}^2}\right), \end{aligned} \quad (15)$$

where $\text{M}(a, b, z) = 1/(\Gamma(a)\Gamma(b-a)) \int_0^1 e^{zt} t^{a-1} (1-t)^{b-a-1} dt$ is Kummer's confluent hypergeometric function, which is implemented in standard numerical mathematics libraries (note that the term $\Gamma(p+q+1/2)$ in the numerator is omitted in Gravestock, Held, and COMBACTE-Net consortium [29]).

Combining the joint prior $\pi(\theta_T, \gamma \mid \mathbf{D}_S)$ with the likelihood of the target study data produces a joint posterior for θ_T and γ , that is,

$$\begin{aligned} \pi(\theta_T, \gamma \mid \mathbf{D}_T, \mathbf{D}_S) &= \frac{\mathcal{L}(\mathbf{D}_T \mid \theta_T) \pi(\theta_T, \gamma \mid \mathbf{D}_S)}{\int_0^1 \int_{-\infty}^{\infty} \mathcal{L}(\mathbf{D}_T \mid \theta'_T) \pi(\theta'_T, \gamma' \mid \mathbf{D}_S) d\theta'_T d\gamma'} \\ &= \frac{\mathcal{N}(\hat{\theta}_T \mid \theta_T, \sigma_{\theta_T}^2) \mathcal{N}(\theta_T \mid \hat{\theta}_S, \sigma_{\theta_S}^2 / \gamma) \text{Be}(\gamma \mid p, q)}{\int_0^1 \mathcal{N}(\hat{\theta}_T \mid \hat{\theta}_S, \sigma_{\theta_T}^2 + \sigma_{\theta_S}^2 / \gamma') \text{Be}(\gamma' \mid p, q) d\gamma'}, \end{aligned} \quad (16)$$

from which a marginal posterior for γ can be obtained by integrating out θ_T , that is,

$$\begin{aligned} \pi(\gamma \mid \mathbf{D}_T, \mathbf{D}_S) &= \int_{-\infty}^{+\infty} \pi(\theta_T, \gamma \mid \mathbf{D}_T, \mathbf{D}_S) d\theta_T \\ &= \frac{\mathcal{N}(\hat{\theta}_T \mid \hat{\theta}_S, \sigma_{\theta_T}^2 + \sigma_{\theta_S}^2 / \gamma) \text{Be}(\gamma \mid p, q)}{\int_0^1 \mathcal{N}(\hat{\theta}_T \mid \hat{\theta}_S, \sigma_{\theta_T}^2 + \sigma_{\theta_S}^2 / \gamma') \text{Be}(\gamma' \mid p, q) d\gamma'} \\ &\propto \mathcal{N}(\hat{\theta}_T \mid \hat{\theta}_S, \sigma_{\theta_T}^2 + \sigma_{\theta_S}^2 / \gamma) \text{Be}(\gamma \mid p, q). \end{aligned} \quad (17)$$

The posterior distribution of the power parameter can therefore be approximated using numerical integration.

Moreover, Gravestock, Held, and COMBACTE-Net consortium [29] show that:

$$\begin{aligned} \pi(\theta_T \mid \mathbf{D}_T, \mathbf{D}_S) &= C(\gamma) \int_0^1 \mathcal{N}(\hat{\theta}_T \mid \theta_T, \sigma_{\theta_T}^2) \mathcal{N}(\theta_T \mid \hat{\theta}_S, \sigma_{\theta_S}^2 / \gamma) \text{Be}(\gamma \mid p, q) d\gamma \\ &\propto \exp\left(-\frac{(\hat{\theta}_T - \theta_T)^2}{2\sigma_{\theta_T}^2}\right) \text{M}\left(\frac{1}{2} + p, \frac{1}{2} + p + q, -\frac{(\hat{\theta}_S - \theta_T)^2}{2\sigma_{\theta_S}^2}\right). \end{aligned} \quad (18)$$

When implementing this model, we took inspiration from the code in Pawel, Aust, Held, and Wagenmakers [48], which relies on numerical integration instead of the full analytical expression that includes the confluent hypergeometric function. We noticed that computing the posterior using the full analytical expression was faster than using numerical integration. However, when using adaptive quadrature to compute the mean and variance of the distribution, using numerical integration to obtain the posterior density led to a much faster computation compared to using the full analytical expression, yet with similar accuracy. Therefore, we instead relied on numerical integration to compute the posterior distribution. To better interpret this prior, we reparameterize it as $\gamma \sim \text{Beta}(\xi_\gamma / \omega_\gamma, (1 - \xi_\gamma) / \omega_\gamma)$, where $\mathbb{E}[\gamma] = \xi_\gamma$ and $\mathbb{V}[\gamma] = \sigma_\gamma^2 = \frac{\omega_\gamma \xi_\gamma (1 - \xi_\gamma)}{1 + \omega_\gamma}$. We used $\xi_\gamma = 0.5$, and vary ω_γ so that the standard deviation of the Beta prior ranges from 0 to 0.50. We have: $\omega_\gamma = \frac{\sigma_\gamma^2}{\xi_\gamma(1 - \xi_\gamma) - \sigma_\gamma^2}$.

A.3 Estimation of posterior distributions

Markov Chain Monte Carlo In the Bayesian framework, all information about the target treatment effect is summarized in the posterior distribution $p(\theta_T \mid \mathbf{D}_S = d_S, \mathbf{D}_T = d_T)$. In many cases, however, this posterior distribution cannot be computed analytically, but several methods exist to approximate it. In the simulation study, when possible, we relied on numerical integration to compute the posterior distribution, or on Markov chain Monte Carlo (MCMC) simulation techniques to draw approximate samples from the posterior distribution. These samples then allowed us to estimate quantities of interest, such as the posterior mean, median, and other quantiles.

We used the probabilistic programming language Stan for running MCMC. Given that all parameters in the models are continuous, we used the default sampler in Stan, the No-U-Turn Sampler (NUTS, Hoffman and Gelman [49]), an advanced and highly efficient MCMC sampling algorithm. Unless required because of convergence issues or strong autocorrelation, we used Stan's default parameters for NUTS.

Number of chains Using multiple chains with random initial values makes the convergence diagnostic more accurate (see Section A.3), and is safer in situations where the posterior distribution is multi-modal. That is, it mitigates the risk of having the chain circumscribed around a mode, and potentially allows identifying multimodality. This can lead to a better approximation of the posterior, even if between-chain mixing is not achieved. As a consequence, we used 4 chains.

Initial values Treatment effect parameters and hyperparameters were initialized by taking samples from their respective prior (or hyperprior) distributions.

MCMC Effective Sample Size The MCMC effective sample size (MCMC ESS) represents the number of independent samples from the posterior distribution that provide the same amount of information as the correlated draws generated by MCMC. In other words, it quantifies the efficiency of the MCMC algorithm in exploring the posterior distribution. An MCMC ESS is estimated for each parameter. Aiming for a sufficiently large MCMC ESS is crucial for reliable estimation.

Moreover, a crucial quantity estimated from MCMC draws is $\Pr(\theta_T \notin \Theta_0)$. Indeed, it is concluded that the treatment is effective if $\Pr(\theta_T \notin \Theta_0) > \eta$, with $\eta = 0.975$. Therefore, we need to ensure that we get a precise estimate of the 0.975th sample quantile.

The reasoning used to determine the standard deviation of sample quantiles is given in appendix 5.2, allowing us to conclude that if we want the 0.975th sample quantile to be estimated with the same precision as the median, we would need $1/0.47 = 2.14$ times more samples.

Based on these considerations, we ensured that the MCMC effective sample size for the target trial treatment effect parameter θ_T is at least 10,000 and adapt the chains' length consequently. Assuming a posterior that is a standard normal distribution, this would correspond to a standard error on the median estimate of 0.0125, and a standard error on the 0.975th sample quantile estimate of 0.0267. Concretely, with $N_C = 4$ chains of length L , for each simulated data replicate, we computed the MCMC ESS for the target treatment effect ϵ_{θ_T} . We then adjusted the chain length so that $L \leftarrow 1.1 \times L \times \epsilon_{\theta_T} / \epsilon$, where ϵ is the target MCMC ESS of 10,000, and repeated the iteration until sufficient MCMC, that is, until $\epsilon_{\theta_T} > \epsilon$. To avoid an explosion of chains length, we capped L to 10,000. By contrast, for speed gains, we reduced chain lengths when $\epsilon_{\theta_T} > 1.1 \times \epsilon$, applying $L \leftarrow 1.1 \times L \times \epsilon_{\theta_T} / \epsilon$, and proceeded to the next data replicates.

Convergence diagnostics By definition, a Markov chain generates samples from the target distribution only after it has converged to equilibrium. In theory, convergence is only guaranteed asymptotically, therefore, in practice, diagnostics must be applied to monitor convergence for the finite number of draws actually available. Therefore, at the model development stage, when using MCMC, Markov Chains visual inspection was performed using tools such as trace plots and autocorrelation plots to verify that the MCMC chains have reached a stationary distribution. To automate the MCMC convergence diagnostic for each replicate, we used the Gelman and Rubin (1992) potential scale reduction statistic \hat{R} to monitor convergence. \hat{R} measures the ratio of the average variance of samples within each chain to the variance of the pooled samples across chains. If all chains are at equilibrium, these will be the same and \hat{R} will be one, and greater otherwise. Gelman and Rubin's recommendation is that the independent Markov chains be initialized with diffuse starting values for the parameters and sampled until all values for \hat{R} are below 1.1. We also monitored the number of transitions ending with a divergence.

Execution of the code does not stop in case of issues with MCMC inference; rather, a warning is stored in the results table so that the pipeline is not interrupted. In case of convergence issues, we adapted the MCMC algorithm by increasing the acceptance probability of the sampler, the tuning period, and reparameterizing the distribution. These convergence diagnoses also allowed us to determine if some models have particular behaviors that need specific handling.

A.3.1 Standard deviation of the sample quantiles

To determine the standard deviation of sample quantiles, we follow the following reasoning: let Y be a continuous random variable with probability density function f , for which we have a sample of size n . We are interested in determining the distribution of the sample median and 0.975th quantile, denoted X_q (with $q_1 = 0.5$ and $q_2 = 0.975$ respectively). We adapt the reasoning developed by Dr William A. Huber in <https://stats.stackexchange.com/a/86804/919>.

Let's denote G_q the c.d.f. of $Beta(\alpha, \beta)$, with $\alpha = qn + 1$ and $\beta = (1 - q)n + 1$. Then, the c.d.f. of X_q in x is $G_q(F(x))$, so that the p.d.f. of X_q is: $\frac{\partial G_q \circ F}{\partial x}(x) = g_q(F(x))f(x)$.

So the p.d.f. of the sample quantile is $g_q(F(x))f(x)$.

Now we are interested in approximating the variance of this distribution.

By denoting $\mu_q = F^{-1}(q)$, we have, for sufficiently well-behaved F :

$$\begin{aligned}
 F(x) &= F(\mu_q + (x - \mu_q)) \\
 &\approx F(\mu_q) + F'(\mu_q)(x - \mu_q) \\
 &\approx q + f(\mu_q)(x - \mu_q)
 \end{aligned} \tag{19}$$

So, assuming f is continuous near μ_q , the p.d.f. of X_q is approximately : $g_q(q + f(\mu_q)(x - \mu_q))f(\mu_q)$. This is essentially a shift of the location and scale of the Beta distribution. The variance of $Beta(\alpha, \beta)$ is :

$$\frac{\alpha\beta}{(\alpha + \beta)^2(\alpha + \beta + 1)},$$

so that the variance of the sample quantile is approximately:

$$\frac{\alpha\beta}{(\alpha + \beta)^2(\alpha + \beta + 1)f(F^{-1}(q))^2},$$

So, for large n , this variance can be approximated as : $\frac{q(1-q)}{nf(F^{-1}(q))^2}$. So for two different quantiles q_1 and q_2 , the ratio of standard error on the sample quantile is approximately :

$$\sqrt{\frac{q_1(1-q_1)}{q_2(1-q_2)} \frac{f(F^{-1}(q_2))}{f(F^{-1}(q_1))}}$$

For the standard normal distribution, with $q_1 = 0.5$ and $q_2 = 0.975$, this gives a ratio of 0.47.

B Supplementary tables

N_T	Botox	Dapagliflozin	Aprepitant	Belimumab	Teriflunomide	Mepolizumab
N_S	468	267	573	577	761	551
$N_S/2$	234	133	286	289	381	275
$N_S/4$	117	66	143	144	190	137
$N_S/6$	78	44	95	96	95	91

Table S1: Table summarizing the total sample sizes considered for the target study, in each case study.

Case study	Drift range	Drift with $\theta_T^{(true)} = \theta_0$	Treatment effect range
Belimumab	[-1.02,1.02]	-0.48	[-0.541,1.5]
Botox	[-0.365,0.365]	-0.2	[-0.165,0.565]
Dapagliflozin	[-0.707,0.707]	-0.36	[-0.347,1.07]
Mepolizumab	[-1.53,1.53]	0.693	[-2.23,0.839]
Aprepitant	[-0.657,0.343]	-0.132	[-0.526,0.474]
Teriflunomide	[-0.588,0.588]	0.411	[-0.999,0.177]

Table S2: Drift ranges considered for each case study.

Metric	Design prior		
Average TIE	Truncated analysis prior	Truncated UI prior	Truncated source posterior
Prior proba. of no treatment benefit	Analysis prior	UI prior	Source posterior
Pre-posterior proba. of FP			
Upper bound on the proba. of FP			

Table S3: Summary of design priors used to compute Bayesian OCs related to type I error.

Metric	Design prior		
Average power	Truncated analysis prior	Truncated UI prior	Truncated source posterior
Prior probability of study success	Analysis prior	UI prior	Source posterior
Pre-posterior proba. of FP			

Table S4: Summary of design priors used to compute Bayesian OCs related to power.

Metric	Definition
Average TIE	$\int Pr(\text{Study success} \theta_T) \frac{\pi(\theta_T \mathbf{D}_S=d_S)\mathbf{I}\{\theta_T \leq \theta_0\}}{Pr(\theta_T \leq \theta_0)} d\theta_T$
Prior proba. of no treatment benefit	$Pr(\theta_T \leq \theta_0)$
Pre-posterior proba. of false positive	$Pr(\text{Study success}, \theta_T \leq \theta_0) = \int_{\theta_T \leq \theta_0} Pr(\text{Study success} \theta_T) p_d(\theta_T) d\theta_T$
Upper bound on the proba. of false positive	$Pr(\text{Study success} \theta_T = \theta_0) \times Pr(\theta_T \leq \theta_0)$

Table S5: Summary of Bayesian OCs related to type I error.

Metric	Definition
Average power	$\int Pr(\text{Study success} \theta_T) \frac{\pi(\theta_T \mathbf{D}_S=d_S)\mathbf{I}\{\theta_T > \theta_0\}}{Pr(\theta_T > \theta_0)} d\theta_T$
Prior probability of study success	$Pr(\text{Study success}) = \int Pr(\text{Study success} \theta_T) p_d(\theta_T) d\theta_T$
Pre-posterior probability of true positive	$Pr(\text{Study success}, \theta_T > \theta_0) = \int_{\theta_T > \theta_0} Pr(\text{Study success} \theta_T) p_d(\theta_T) d\theta_T$

Table S6: Summary of Bayesian OCs related to power.

Method	Fixed parameters/Priors	Parameters to vary	Range of variation
Test-then-pool, equivalence test	None	Significance level of the equivalence test η . Equivalence margin λ .	$\eta \in \{0.1, 0.5\}$, $\lambda \in \{0.1, 0.5, 0.8\}$
Test-then-pool, difference test	None	Significance level of the difference test η	$\eta \in \{0.1, 0.5\}$
Conditional power prior (PP)	Initial prior on θ	Power parameter γ	$\gamma \in \{0, 0.25, 0.5, 0.75, 1\}$
Normalized PP	Initial prior on θ $\gamma \sim \text{Beta}(\xi_\gamma/\omega_\gamma, (1 - \xi_\gamma)/\omega_\gamma)$. $\xi_\gamma = 0.5$	ω_γ	ω_γ is varied so that the standard deviation of the Beta prior ranges from 0 to 0.50
Empirical Bayes PP	Initial prior on θ	None	None
p -value based PP	Initial prior on θ	Shape parameter k	$k \in \{0.01, 0.1, 1, 10, 20\}$
Commensurate PP	Initial prior on θ_S	Prior on the commensurability parameter τ	See the text
Robust mixture prior	Variance of the vague component	Mixture weight w .	w in a grid of values ranging from 0 to 1 in steps of 0.1.

Table S7: Methods and parameters considered in the simulation study. When the method is based on a consistency assumption ($\theta_T = \theta_S$), we denote the treatment effect as θ .

Disease	Lower limb spasticity	Type-2 diabetes	Postoperative nausea and vomiting	Systemic Lupus Erythematosus (SLE)	Multiple Sclerosis	Severe Eosinophilic Asthma
Drug	Botox vs placebo	Dapagliflozin vs placebo (+ Metformin)	Aprepitant vs ondansetron	Belimumab vs placebo	Teriflunomide vs placebo	Mepolizumab vs placebo
Endpoint	Disease severity score	Glycated hemoglobin HbA1c	Absence of vomiting and rescue therapy 0-24h after surgery	SLE Responder Index	Time to first relapse	Number of clinically significant exacerbations.
Endpoint type	Continuous	Continuous	Binary	Binary	Time to event	Recurrent event
Summary measure	Difference in mean scores between the two arms	Difference between the two arms in change in HbA(1c) scores from baseline to week 24/26	Difference in response rates between the two arms	Log odds ratio for active treatment compared to placebo	Log hazard ratio for active treatment compared to placebo	Log exacerbation rate ratio for active treatment compared to placebo
Treatment effect distribution	Normal	Normal	Integral of the product of binomials	Normal (approximation for the log OR)	Normal (approximation for the log HR)	Normal (approximation for the log rate ratio)
N_T : ctrl/trt/tot	130/126/256	76/81/157	52/55/107	39/53/92	57/109/166	NA/NA/25
N_S : ctrl/trt/tot	235/233/468	134/133/267	293/280/573	562/563/1125	752/731/1483	NA/NA/551
y_T /Data	0.10 (0.10)	1.03 (95% CI, 0.49-1.57) (at week 26)	Treatment : 48/55, control: 42/52	Treatment : 28 /53 Placebo: 17/39	HR : 0.66 (95% CI, 0.39-1.11)	Rate ratio : 0.67 (0.17, 2.68)
y_S /Data	0.20 (0.10)	0.36 (0.102) (at week 24)	Treatment : 184/293 Control : 154/280	Treatment: 285/563 Placebo: 218/562	HR : 0.68 (95% CI, 0.58-0.79)	Rate ratio : 0.50 (0.39, 0.64)
Reference	Wang, Travis, and Gajewski [5]	Shehadeh et al. [6], Bailey, Gross, Pieters, Bastien, and List [7]	Jin, Li, and Kaur [12], Salman, DiCristina, Chain, and Afzal [14], Diemunsch et al. [13]	Best, Ajimi, Neuenschwander, Saint-Hilary, and Wandel [4], Psioda and Xue [9], Brunner et al. [10], Brunner et al. [50]	Bovis, Ponzano, Signori, Schiavetti, Bruzzi, and Sormani [17]	Best, Price, Pouliquen, and Keene [20], MENSA trial [21], Keene, Best, Price, and Pouliquen [22]

Table S8: Table summarizing the case studies used to inspire the simulation study design

Method	Case	Likelihood	# replicates	# drift values	N_S/N_T	Denom. change factor	σ_T/σ_S
EBPP	Botox/Dapagliflozin	Normal	5000	33	1, 2, 4, 6	NA	1, 2
	Belimumab/Mepolizumab/Teriflunomide	Normal	5000	33	1, 2, 4, 6	1/2, 1, 3/2	NA
	Aprepitant	Normal	5000	33	1, 2, 4, 6	NA	NA
NPP	Botox/Dapagliflozin	Normal	1000	23	2, 4	NA	1
	Belimumab/Mepolizumab/Teriflunomide	Normal	1000	23	2, 4	1	NA
	Aprepitant	Normal	1000	23	2, 4	NA	NA
Comm. PP	Botox/Dapagliflozin	Normal	1000	23	2, 4	NA	1
	Belimumab/Mepolizumab/Teriflunomide	Normal	1000	23	2, 4	1	NA
	Aprepitant	Normal	1000	23	2, 4	NA	NA
Others	Botox/Dapagliflozin	Normal	5000	33	1, 2, 4, 6	NA	1, 2
	Belimumab/Mepolizumab/Teriflunomide	Normal	5000	33	1, 2, 4, 6	1/2, 1, 3/2	NA
	Aprepitant	Binomials	1000	23	2, 4	NA	NA

Table S9: Light configuration used in the simulation study for all drift values. Other methods include separate analysis, pooling, RMP, CPP, and Test-then-Pool (equivalence test or difference test).

Method	Case	Likelihood	# replicates	# drift values	N_S/N_T	Denom. change factor	σ_T/σ_S
EBPP	Botox/Dapagliflozin	Normal	10000	3	1, 2, 4, 6	NA	1, 2
	Belimumab/Mepolizumab/Teriflunomide	Normal	10000	3	1, 2, 4, 6	$1/2, 1, 3/2$	NA
	Aprepitant	Normal	10000	33	1, 2, 4, 6	NA	NA
NPP	Botox/Dapagliflozin	Normal	10000	3	2, 4	NA	1
	Belimumab	Normal	10000	3	2, 4	1	NA
	Mepolizumab/Teriflunomide	Normal	8000	3	2, 4	1	NA
	Aprepitant	Normal	10000	3	2, 4	NA	NA
Comm. PP	Botox/Dapagliflozin	Normal	10000	3	4	NA	1
	Belimumab/Mepolizumab/Teriflunomide	Normal	10000	3	4	1	NA
	Aprepitant	Normal	10000	3	4	NA	NA
Others	Botox/Dapagliflozin	Normal	10000	3	1, 2, 4, 6	NA	1, 2
	Belimumab/Mepolizumab/Teriflunomide	Normal	10000	3	1, 2, 4, 6	$1/2, 1, 3/2$	NA
	Aprepitant	Binomials	10000	3	4	NA	NA

Table S10: Compute-intensive configuration used in the simulation study for the three main treatment effect values. Other methods include separate analysis, pooling, RMP, CPP, and Test-then-Pool (equivalence test or difference test).

C Supplementary figures

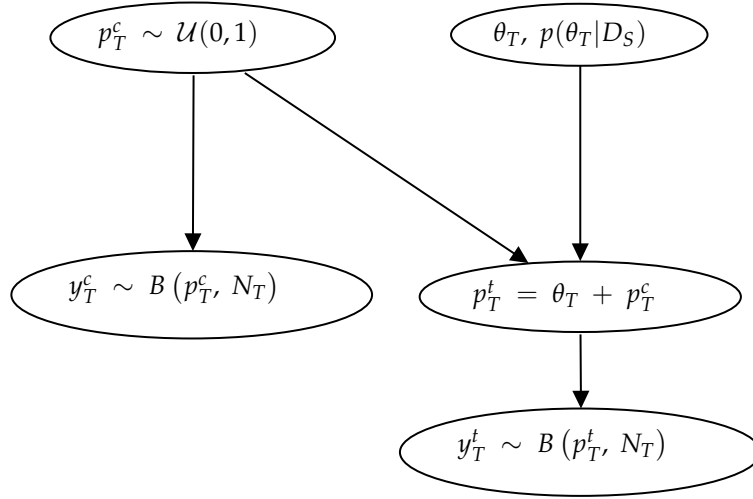


Figure S1: Structure of the model in case where the likelihood is a product of binomials.

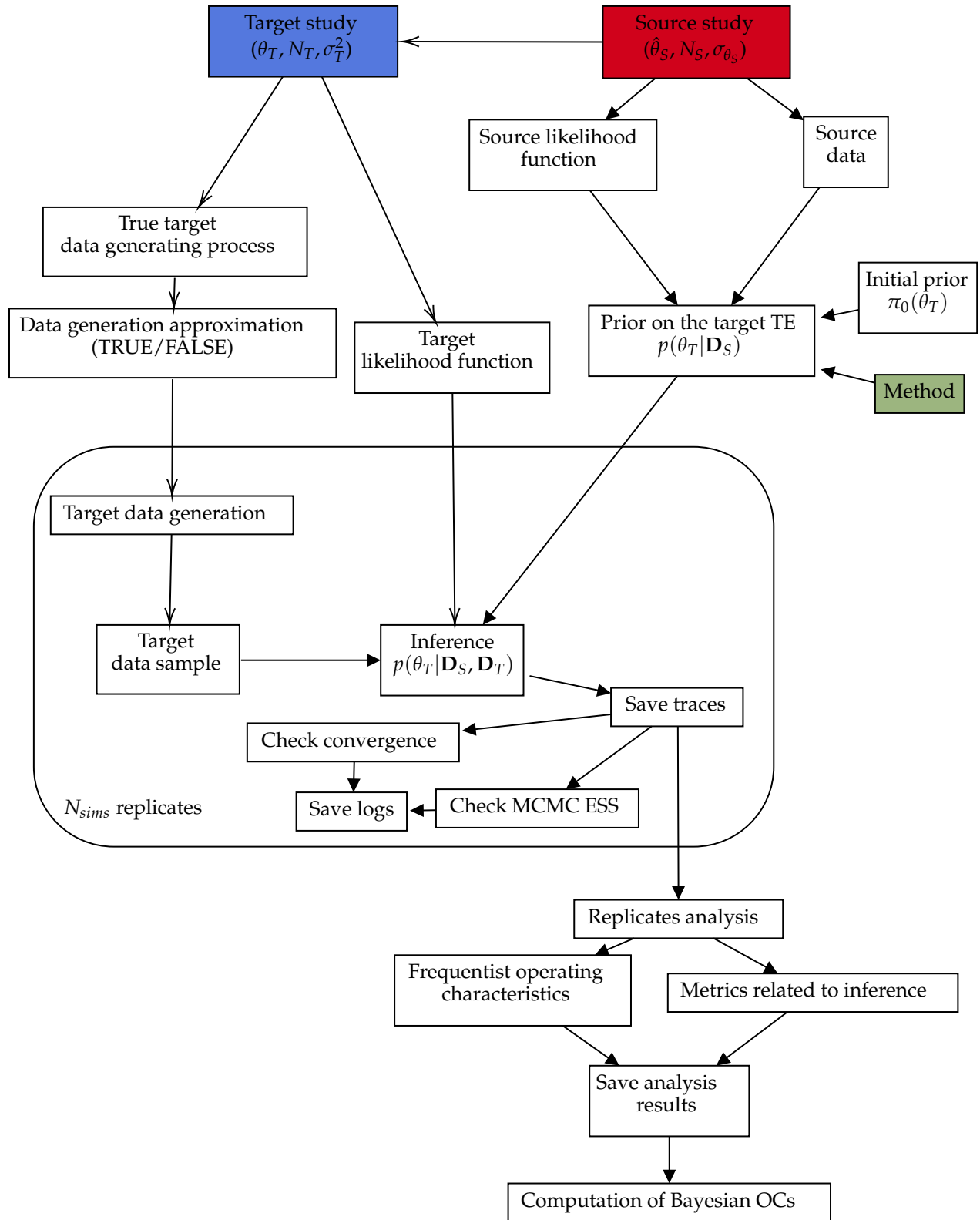


Figure S2: Summary of the simulation study pipeline. Colored boxes correspond to components of the configuration that will be varied.

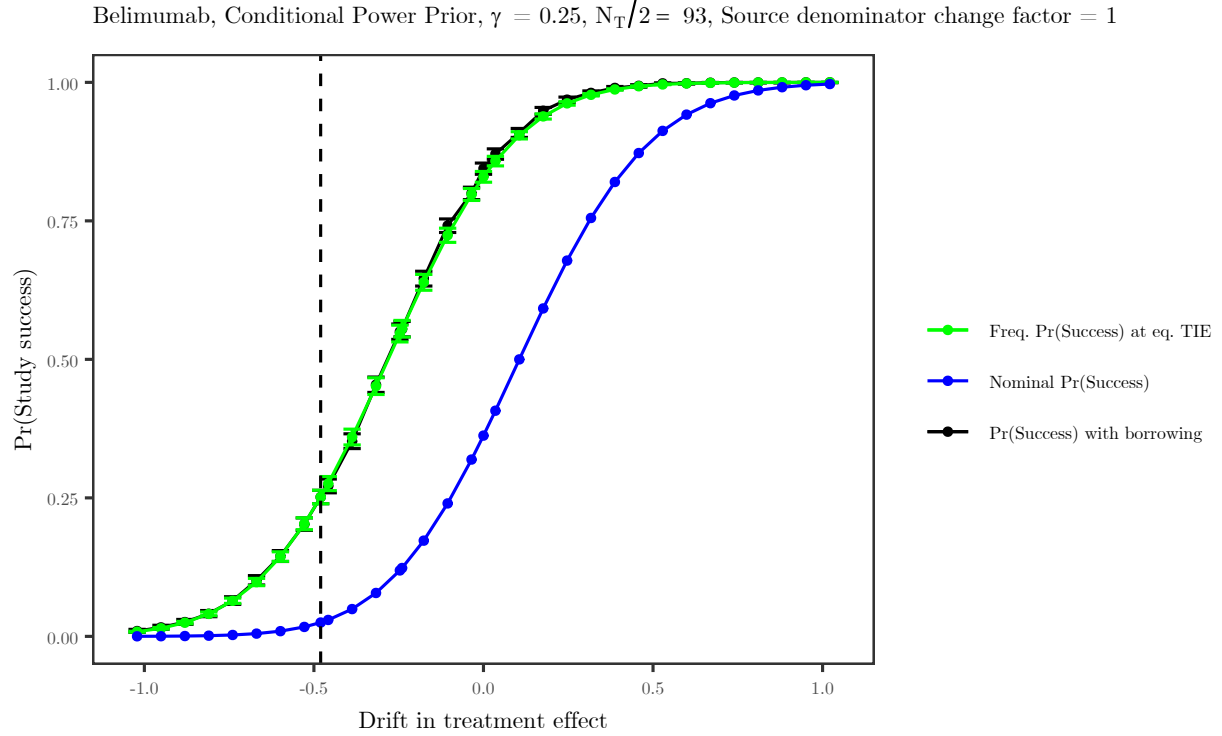


Figure S3: Probability of success of the Conditional Power Prior with $\gamma = 0.25$ as a function of the drift in treatment effect (black) in the Belimumab case study at a sample size per arm of 93, without change introduced in the denominator of the source study summary measure. The probability of success of the t-test at a nominal type 1 error rate of 0.025 as a function of drift is displayed in blue. The probability of success of the t-test at a type 1 error rate equal to the Conditional PP type 1 error rate is displayed in green. Borrowing of external data that favors the null hypothesis also implies that the probability of success of the borrowing method is always larger, in the alternative hypothesis space, than the probability of success of the frequentist method at the nominal type 1 error rate of 0.025. The power curves at equivalent type 1 error rate are identical. $\theta_T = \theta_0$ is indicated by a dashed line. Error bars correspond to the 95% Confidence Interval of the metric.

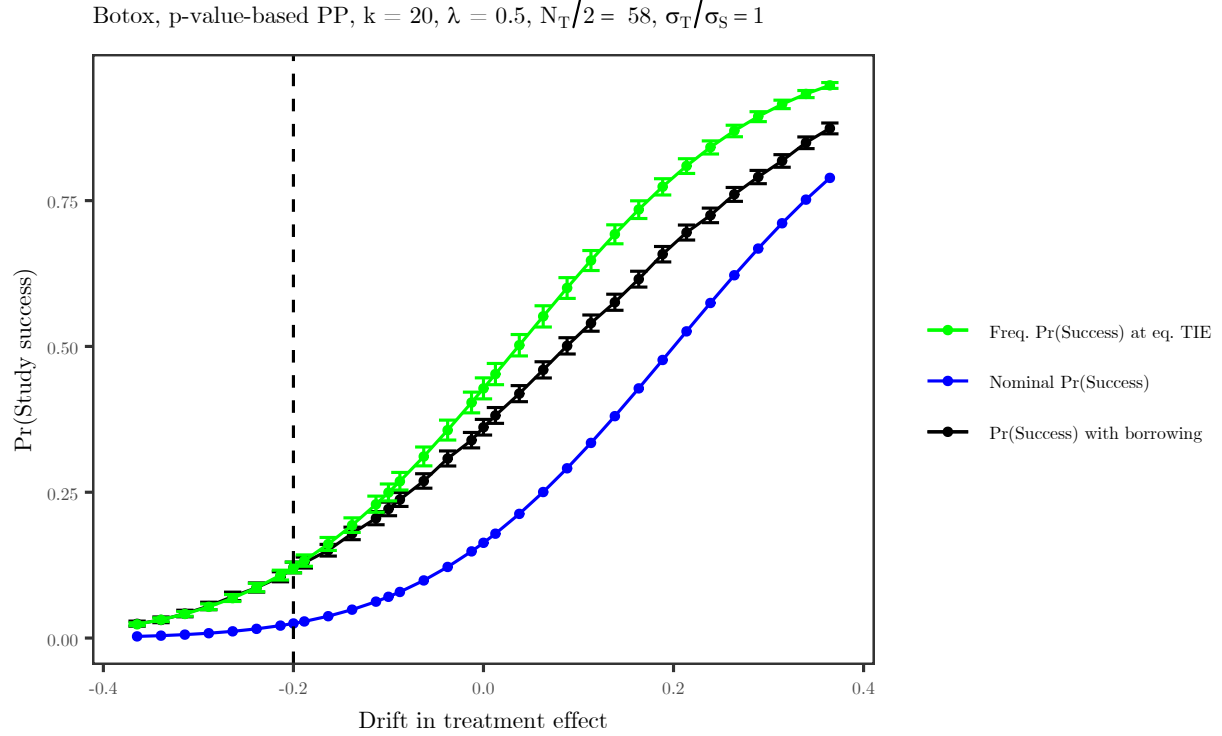


Figure S4: Probability of success of the p-value-based Power Prior with parameters $k = 20$ and $\lambda = 20$ as a function of the drift in treatment effect (black) in the Botox case study at a sample size per arm of 58, with a sampling standard deviation equal between the source and target study. The probability of success of the t-test at a nominal type 1 error rate of 0.025 as a function of drift is displayed in blue. The probability of success of the t-test at a type 1 error rate equal to the p-value based PP type 1 error rate is displayed in green. $\theta_T = \theta_0$ is indicated by a dashed line. In this example, the power of the p-value based power prior is lower than the power of the frequentist t-test at equivalent type 1 error rate in the whole alternative hypothesis space. Error bars correspond to the 95% Confidence Interval of the probability of success.

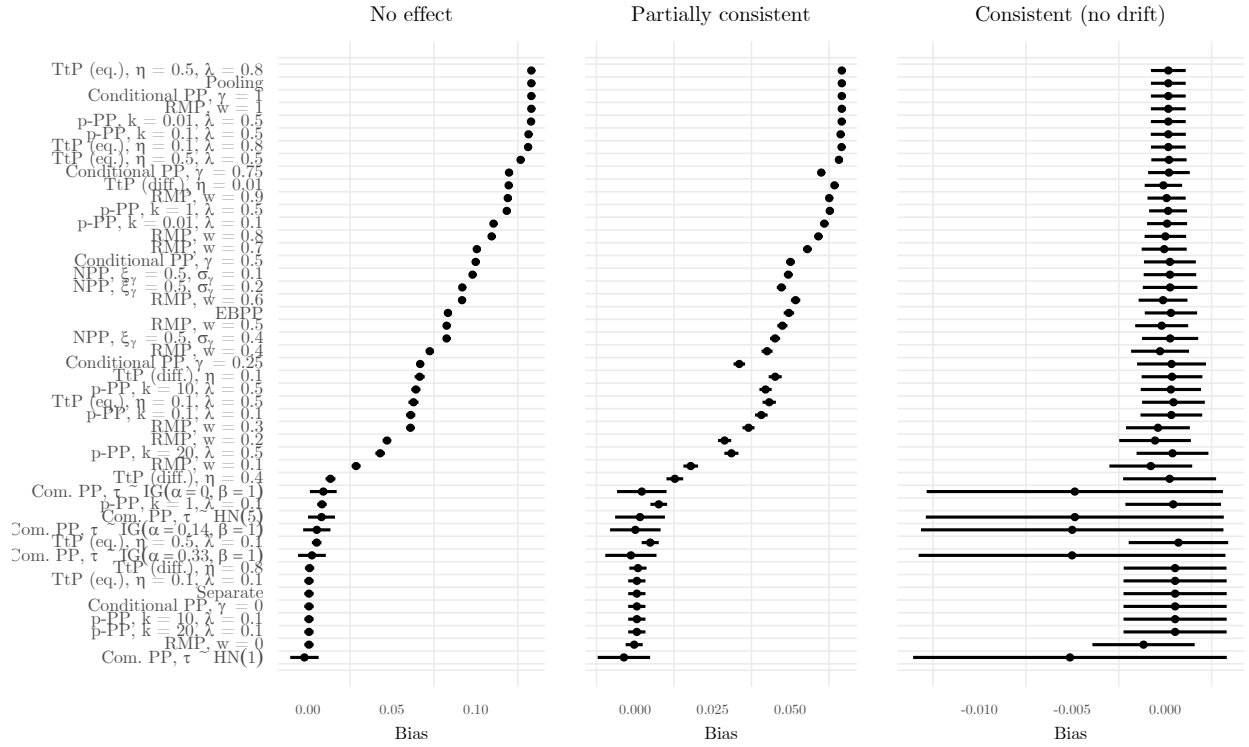


Figure S5: Comparison of the bias of the different methods and associated 95% CI, for the three main treatment effects considered, in the Botox case study with 117 samples per arm in the target trial. The ordering of methods is made with respect to the bias in the absence of effect.

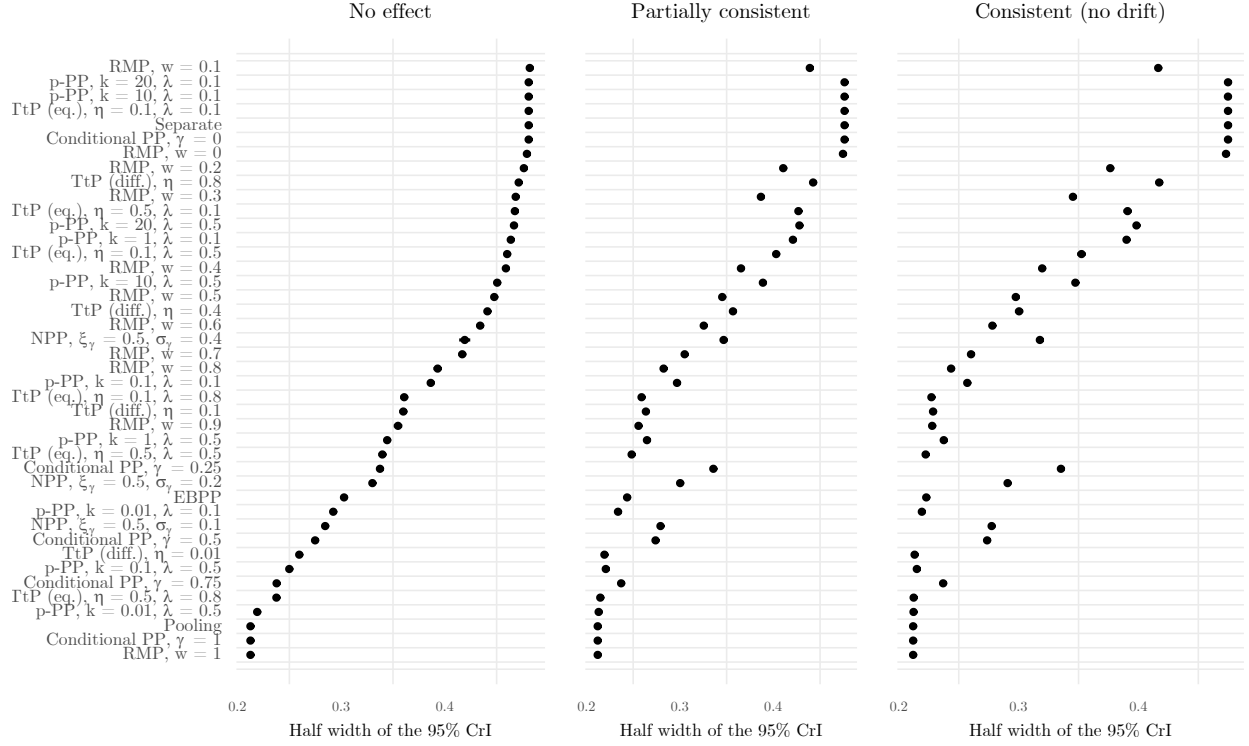


Figure S6: Comparison of the precision, measured as the mean half-width of the 95% Credible Interval, of the different methods for the three main treatment effect values considered in the Belimumab case study. Error bars correspond to the 95% Confidence Interval of the precision. The ordering of methods is made with respect to the precision in the absence of effect.

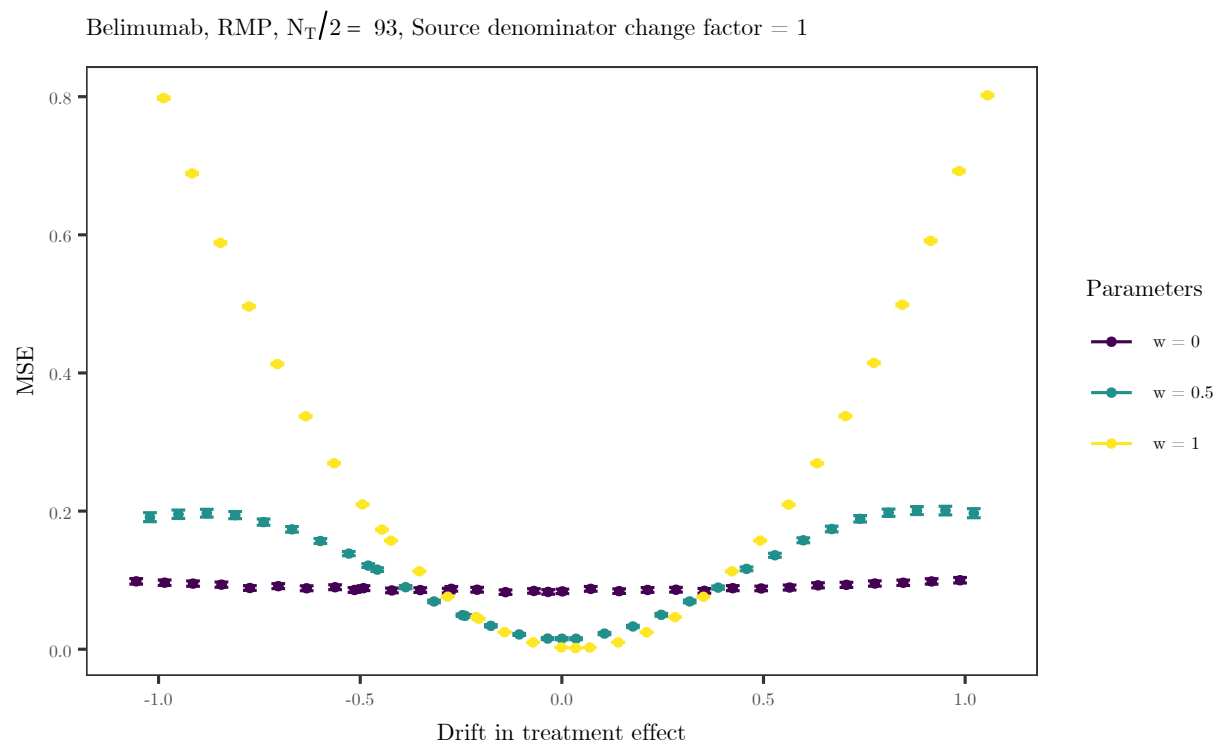


Figure S7: MSE as a function of drift for the RMP in the Belimumab case study, with a sample size per arm in the target study of 93 patients, for different values of the weight of the informative component w . Error bars correspond to the 95% Confidence Interval of the MSE.

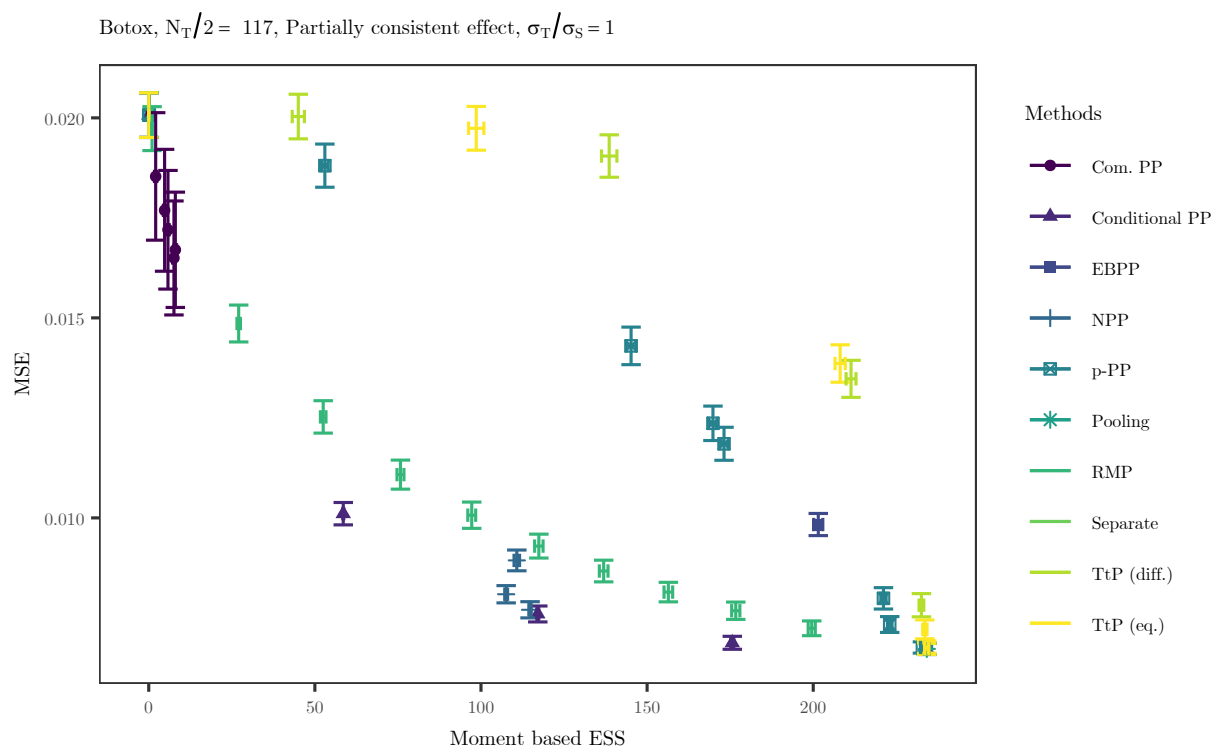


Figure S8: MSE as a function of the mean moment-based ESS in the Botox case study with a sample size per arm of 117. Error bars correspond to the 95% Confidence Interval of the MSE

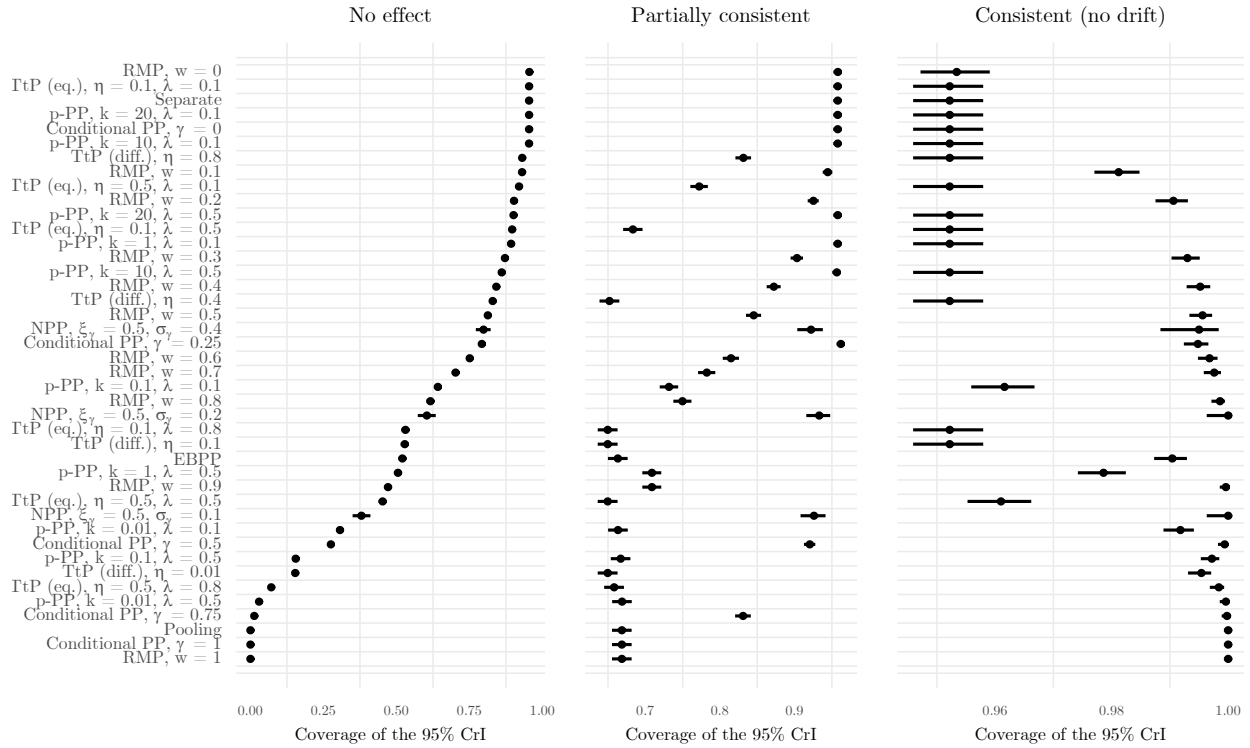


Figure S9: Comparison of the coverage probability of the 95% of the different methods for the three main treatment effect values considered in the Belimumab case study. Error bars correspond to the 95% Confidence Interval on the coverage probability. The ordering of methods is made with respect to the coverage in the absence of effect.

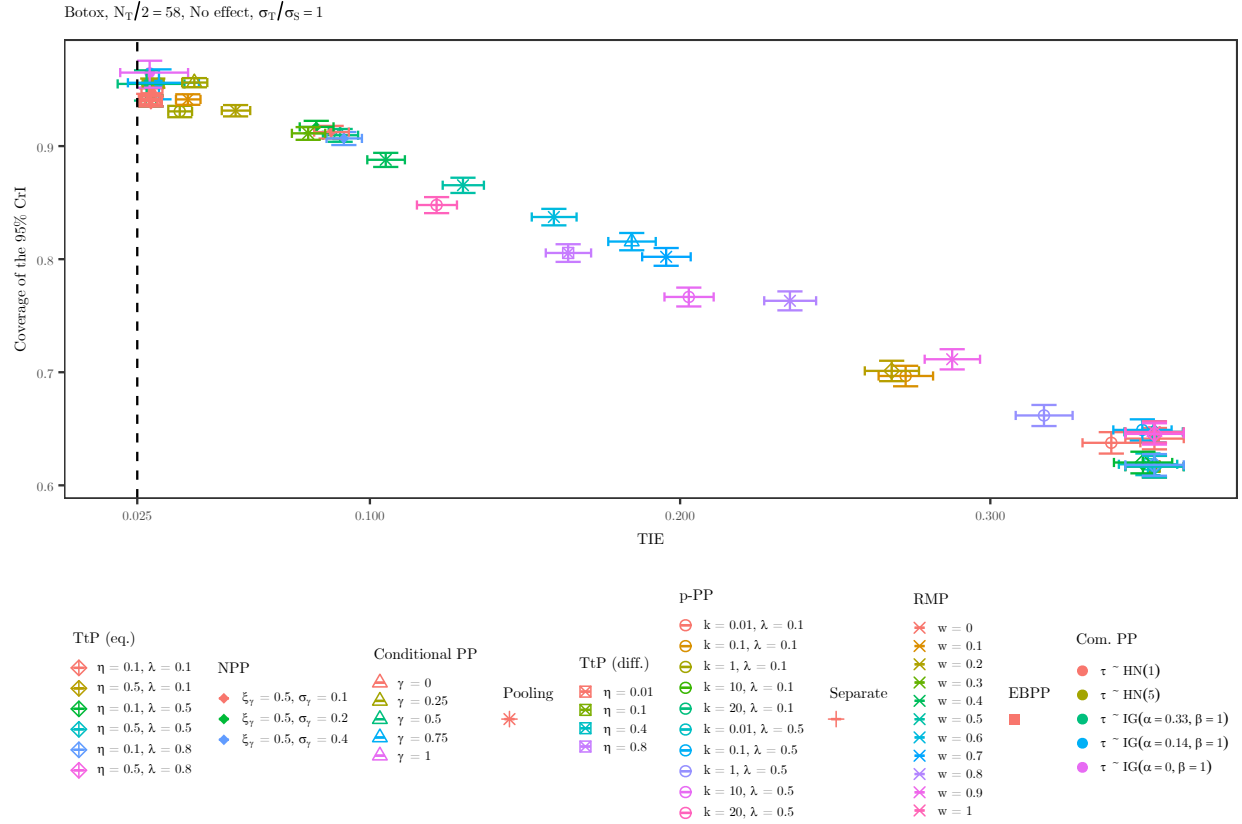


Figure S10: Coverage of the 95% Confidence Interval as a function of type 1 error rate in the Botox case study with a sample size per arm of 58, across all the methods and parameters, without treatment effect. The target to source standard deviation ratio is 1. Error bars correspond to the 95% Confidence Interval of the Coverage and type 1 error rate. Dashed vertical line represents the nominal type 1 error rate of 0.025.